Preparation and Properties of Glass-Ceramics Containing Ferroelectric Crystals(Dissertation_全文)

AUTHOR(S):

Kokubo, Tadashi

Preparation and Properties of Glass-Ceramics Containing Ferroelectric Crystals

Tadashi KOKUBO

Preparation and Properties of Glass-Ceramics Containing Ferroelectric Crystals

By

Tadashi KOKUBO

TABLE OF CONTENTS

INTRODUCTION

Ceramics with high dielectric constant, for example, barium titanate ($BaTiO_3$) ceramics, are used extensively as various components of electronic devices and conventionally produced by sintering of crystalline powders. If such ceramics are produced by crystallization of glass, that is, through "glass-ceramic process", which consists of melting the raw materials, forming the melts and crystallizing the formed glasses by heat treatment, the following advantages should be expected;

(1) Ceramics of such shapes as thin sheet, fiber and tube, which are difficult to prepare by the conventional method of sintering, can be obtained easily because of good formability of glass.

(2) Ceramics thus obtained are easily sealed together with each other, or with the other ceramics or metals at relatively low temperatures because of low softening temperature of glass and glass-ceramics.

(3) A wide spectrum of dielectric properties can be obtained by controlling the microstructure.

(4) High electrical resistivity and high dielectric strength may result from the pore-free structure.

(5) Ceramics with little aging and low temperature coefficient of dielectric constant are easily obtained by controlling the particle size.

(6) Transparent ceramics may be obtained by controlling

the particle size.

With all these advantages, however, there are two fundamental problems to be considered in the glass-ceramic process; one is the dilution of ferroelectric crystals by non-ferroelectric glass-forming components and the other is complex effects of microstructure on the dielectric properties of the glass-ceramics. To obtain glasses network-forming oxides such as SiO_2, B_2O_3 and Al_2O_3 have to be added to the ferroelectric-crystal components, since the latter alone cannot be vitrified by conventional melting. This necessarily results in the dilution of the ferroelectric crystals by non-ferroelectric components, and the problem arises as to how the amount of precipitated ferroelectric crystals is increased within the given composition range. However, the dielectric constant may not be the function of the amount of the ferroelectric crystals alone; the microstructure of the crystallized glass may be important, too. This requires us to study the effect of microstructure on dielectric constant and to find the way for controlling it.

So far, several works have been published on glass-ceramics of this kind[1-12]. However, few studies have dealt systematically with the fundamental problems encountered in the preparation of high dielectric constant glass-ceramics.

The present paper is the record of the investigations conducted on glass-ceramics with high dielectric constant, for the purpose of finding the principles underlying their preparation. More specifically, the method for preparing the bulk and film glass-ceramics and their dielectric proper-

ties in relation to their microstructure are dealt with. The paper consists of the following two parts:

I. Glass-ceramics in the system $BaO-TiO_2-Al_2O_3-SiO_2$

II. Glass-ceramics in the system $PbO-TiO_2-Al_2O_3-SiO_2$

In general, barium titanate glass-ceramics dealt in PART I are characterized by high dielectric constant, while lead titanate glass-ceramics dealt in PART II are characterized by low softening temperature.

References

1) R.C. Anderson and A.L. Friedberg, Symposium on Nucleation and Crystallization in Glasses and Melts, American Ceramic Society, p. 29 (1962).

2) R.E. Allen and A. Herczog, U.S. Pat. No. 3,114,066, Dec. 10, 1963.

3) A. Herczog, J. Am. Ceram. Soc., 47 107 (1964).

4) A. Herczog and S.D. Stookey, U.S. Pat. No. 3,195,030, July 13, 1965.

5) N.F. Borrelli, A. Herczog and R.D. Maurer, Appl. Phys. Letters, 7 117 (1965).

6) D.R. Ulrich and E.J. Smoke, J. Am. Ceram. Soc., 49 210 (1966).

7) M.M. Layton and A. Herczog, J. Am. Ceram. Soc., 50 369 (1967).

8) N.F. Borrelli, J. Appl. Phys., 38 4243 (1967).

9) L.W. Asher and C.R. Pratt, Jr., Proc. Elec. Component Conf., 239 (1967).

10) A.K. Banerjee and R.L. Thakur, Central Glass. Ceram. Res. Inst. Bull., 15 38 (1968).

11) D.G. Grossman and J.O. Isard, J. Am. Ceram. Soc., 52 230 (1969).

12) M.M. Layton and A. Herczog, Glass Tech., 10 50 (1969).

PART I. GLASS-CERAMICS IN THE SYSTEM $BaO-TiO_2-Al_2O_3-SiO_2$

Chapter 1. Preparation and Properties of the Bulk Glass-Ceramics

Barium titanate ($BaTiO_3$) ceramics, one of the most popular ferroelectric ceramics, exhibit very high dielectric constants among others. Accordingly, the attempt to prepare ferroelectric ceramics by the glass-ceramic process has been started with the composition containing $BaTiO_3$. Herczog[1] initially investigated the crystallization of a series of glasses having the compositions $xBaTiO_3+(100-x)BaAl_2Si_2O_8$ (x by weight) and obtained, from a glass of this system with addition of a small amount of fluoride, a glass-ceramics showing a dielectric constant of 1200. The present author has found, however, that the glass used by Herczog has a high melting temperature and, in addition, tends to devitrify during cooling of the melt. Such behavior is undesirable for preparation of the crystallized glasses (glass-ceramics) with constant dielectric properties.

The present study has started with a search for compositions of glasses that can be melted at relatively low temperatures and also formed without devitrification. Glass formation tendency and crystallization behavior during reheating have been investigated for the composition $(100-x-y)BaO\cdot TiO_2+xAl_2O_3+ySiO_2$, where x and y are varied in the range 0 to 20 and 15 to 60 in mole %, respectively. Also dielectric properties

of the crystallized products have been measured and discussed on the basis of their chemical composition and microstructure.

1. Experimental Procedure

1.1. Preparation of Glasses

To determine the glass formation region in the system $BaO \cdot TiO_2$-Al_2O_3-SiO_2, glasses with the compositions $(100-x-y)BaO \cdot TiO_2 + xAl_2O_3 + ySiO_2$, where x and y were varied in the range of 0 to 20 and 15 to 60 mole %, respectively, were melted. As batch materials were used reagent-grade barium carbonate, titanium oxide and aluminum hydroxide, and high-grade quartz powder of low iron content usually employed in the manufacture of optical glasses. About 50g of the batch mixtures were put in a platinum crucible of 80cc in capacity and melted at 1450°C for 1 hour in an electric furnace. The melt was poured on a steel plate, pressed into the form of plate approximately 2mm thick, and immediately annealed at 650°C in another furnace. Some of the glasses thus obtained, whose compositions are given in Table 1.1, were subjected to the following experiments.

1.2. Differential Thermal Analysis

Crystallization behavior of glass was examined by the differential thermal analysis. A solid cylindrical piece of glass just fit to the DTA sample holder (6mm in diameter and 14mm in height) was used as sample to minimize the effect of the surface crystallization, which might be serious with powder sample. A heating rate of 10°C/min was adopted and α-Al_2O_3 was used as reference material.

Table 1.1. Glass composition

Sample No.	Composition (mole %)		
	$BaO \cdot TiO_2$	Al_2O_3	SiO_2
1	60	20	20
2	60	14	26
3	60	10	30
4	60	6	34
5	63	10	27
6	54	10	36
7	45	10	45

1.3. Crystallization of Glasses

Glass slabs of the size 10x10x1.5mm cut from the plates and ground with No. 2000 Al_2O_3 powder were crystallized by heating on a platinum sheet in an electric furnace. They were heated up at a rate of 5°C/min from room temperature to 1100°C, kept there for 1 hour and cooled in the furnace. The resultant crystallized samples were subjected to the visual observation of the appearance, X-ray diffraction analysis and measurements of dielectric properties.

1.4. X-Ray Diffraction Analysis

Identification of crystal precipitating in the course of crystallization and determination of the amount of $BaTiO_3$ crystals formed in the final crystallized products were conducted by the X-ray diffraction analysis with powdered samples. To determine the $BaTiO_3$ crystal content, intensity of the (101) reflection of $BaTiO_3$ crystals in the sample was measured with the use of the (220) reflection of fluorite

(CaF_2) as an internal standard and compared with a calibration curve. The calibration curve was obtained with intimate mixtures of known amount of $BaTiO_3$ crystals, glass of the composition No. 2 and fluorite crystals. Volume fraction V of the $BaTiO_3$ crystals was calculated from the measured density D_m of the crystallized sample by the formula $V = x(D_m/D)$, where x is the weight fraction determined by the X-ray analysis and $D=6.06 g/cm^3$ is the density of $BaTiO_3$ [2].

1.5. Measurement of Dielectric Properties

Dielectric properties were measured at a frequency of 1Mc/s at room temperature. The measurements were made by a Q-Meter (Type GM-102, Yokogawa Electric Works, Ltd.). Since some of the crystallized glasses showed non-uniform surface, all the samples were ground to rectangular pieces of the size 10x10x1mm to remove the effect of original surfaces. Silver paste applied on both faces of the samples served as electrodes.

2. Results

2.1. Glass Formation Region

Glass formation region in the system $BaO \cdot TiO_2$-Al_2O_3-SiO_2 is shown in Fig. 1.1. The sign o or ⊙ in Fig 1.1 refers to the composition which gave a transparent glass when the melt heated at 1450°C was poured onto a steel plate. Especially the sign ⊙ refers to the glass composition which was used for further investigation. The numbers given correspond to those of the composition given in Table 1.1. The sign △ refers to the composition which did not give an entirely transparent glass due to the formation of scums

at melting temperature or partial devitrification during cooling. The sign x refers to the composition whose melt was completely devitrified during cooling. A solid line L gives a tentative boundary representing a limit of glass formation.

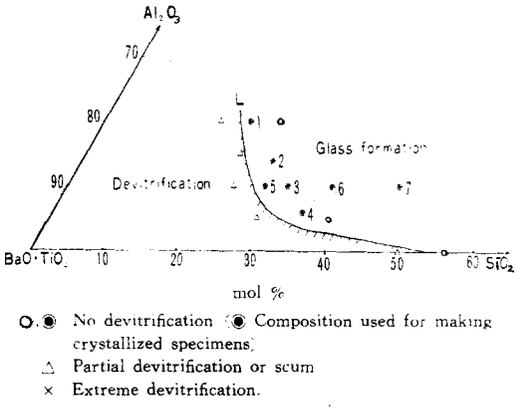

Fig. 1.1. Glass formation region in the system $BaO \cdot TiO_2$-Al_2O_3-SiO_2

2.2. Differential Thermal Analysis and X-Ray Diffraction Analysis

A thermogram of the glass No. 2 ($BaO \cdot TiO_2$ 60, Al_2O_3 14, SiO_2 26 mole %) is given in Fig. 1.2. Two exothermal peaks are observed, one at 850°C and the other at 960°C. Powder X-ray diffraction patterns of the samples heated to the temperatures 900° and 1040°C which are a little over each peak temperature are shown in Fig. 1.3. It is seen from Fig. 1.3(1) that in the sample heated at 900°C a considerable amount of perovskite-type $BaTiO_3$ crystal is precipitated, as indicated by the strong lines designated by x. In addition, there is an unidentified crystalline species to which the lines at 2θ = 18.7°, 25.9°, 28.6°, 32.7°,

37.9°, 39.5° and 43.9° are attributed. In the sample heated at 1040°C (Fig. 1.3(2)), there is a great amount of $BaTiO_3$ crystals and a less amount of the unidentified crystal, as evidenced from the growth and weakening of the corresponding diffraction lines. Further, a series of new diffraction lines designated by the sign o in the figure appears. These lines can be attributed to the hexacelsian ($BaAl_2Si_2O_8$).

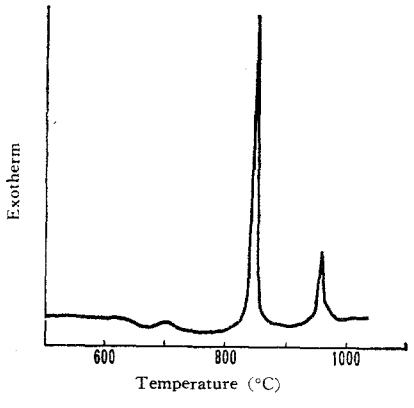

Fig. 1.2. Thermogram of the glass No. 2.

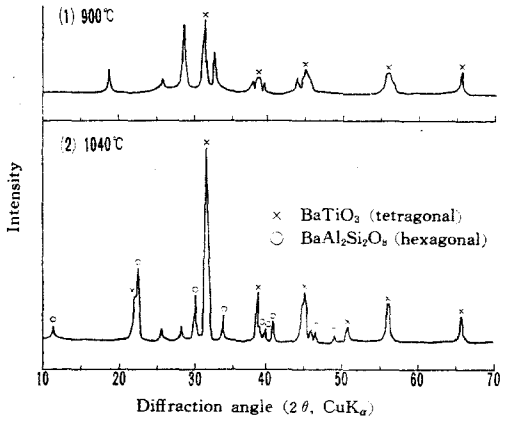

Fig. 1.3. X-ray diffraction patterns of the glass No. 2 heated at 900° and 1040°C.

Herczog[1] also found that the $BaTiO_3$ crystals are precipitated at lower temperatures and then hexacelsian crystals are precipitated at higher temperature in the course of crystallization of the glass having the composition $BaTiO_3$ 74 and $BaAl_2Si_2O_8$ 26 % by weight (BaO 42.4, TiO_2 34.8, Al_2O_3 7.7 and SiO_2 15.1 mole %). No description was made, however, of the unidentified crystal by Herczog.

The kind of crystals and the amount of $BaTiO_3$ crystal found in the samples crystallized by heating to 1100°C by a schedule described in paragraph 1.3 are given in Table 1.2. It can be seen from Table 1.2 that crystals precipitated in the crystallized glasses are perovskite-type $BaTiO_3$, hexacelsian, $BaTiSiO_5$ and unidentified crystals.

2.3. Defects of Crystallized Glasses

The appearance of the crystallized glasses obtained by heating to 1100°C are shown in Fig. 1.4. Although most of the crystallized glasses show no defect, the crystallized sample of the composition No. 1 has a great number of cracks and that of the composition No. 5 has surface ripples.

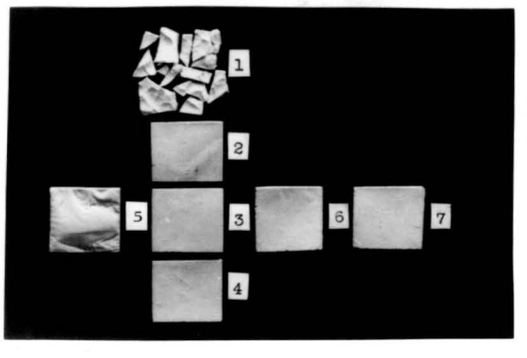

Fig. 1.4. Appearance of crystallized samples obtained by heating up to 1100°C.

Table 1.2. Crystalline phases and dielectric properties

Sample No.	1	2	3	4	5	6	7
Crystalline phases*	BT	BT	BT	BT	BT	BT	-
	BAS	BAS	BAS	BAS	BAS	BAS	BAS
	-	-	BTS	BTS	-	BTS	BTS
	X	X	X	X	X	X	X
Content of $BaTiO_3$ (vol %)	19	23	15	8	18	7	0
Dielectric properties							
Parent glass							
ε	18	17	17	16	17	17	14
tanδ	0.0021	0.0023	0.0020	0.0023	0.0020	0.0022	0.0019
Crystallized product							
ε	168	500	284	77	415	76	23
tanδ	0.0174	0.0250	0.0207	0.0119	0.0304	0.0173	0.0020

* BT ; $BaTiO_3$ (perovskite-type), BAS ; Hexacelsian ($BaAl_2Si_2O_8$), BTS ; $BaTiSiO_5$

X ; Unidentified crystal

In general, the compositions containing too much amount of Al_2O_3 or $BaO \cdot TiO_2$ tend to give the crystallized glasses having defects such as cracks or surface ripples.

2.4. Dielectric Properties

2.4.1. Effects of Heat Treatment

Fig. 1.5 shows the dielectric properties(dielectric constant and tanδ) of the glass No. 2 as a function of temperature of heat treatment. All the measurements were made at room temperature. The glass was heated up at a rate of 5°C/min from room temperature to a temperature (temperature of heat treatment mentioned above) and then taken out immediately from the furnace. It can be seen from the figure that the dielectric constant of the glass first remains almost the same at about 17 up to 700°C and then increases as the temperature of heat treatment is raised. The rate of increase is particularly great in the temperature range from 800° toward 1100°C, where the value reaches 560. The heating up to still higher temperatures affects the dielectric constant only slightly.

Dielectric properties of the same glass kept at 1100°C for various periods are shown in Fig. 1.6. The glass was heated at a rate of 5°C/min from room temperature to 1100°C. The figure shows that both dielectric constant and tanδ do not vary with heating time. In other words, at 1100°C dielectric properties characteristic of the maximum heating temperature (1100°C) are attained as soon as the temperature is reached.

2.4.2. Effects of Chemical Composition

The values of dielectric constant and tanδ of the

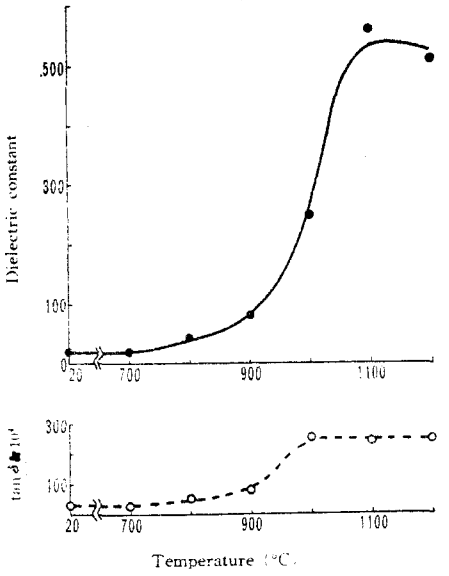

Fig. 1.5. Dependence of dielectric properties upon heating temperature for the glass No. 2.

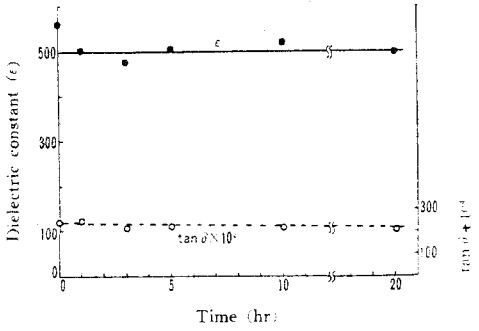

Fig. 1.6. Dependence of dielectric properties upon heating time at 1100°C for the glass No. 2.

crystallized glasses obtained by heating to 1100°C are shown in Table 1.2. The data on the glasses before heat treatment is also shown in the table. The dielectric constants of the crystallized glasses are reproduced in a composition triangle in Fig. 1.7. In this figure the values shown by parentheses represent the amounts (volume fraction) of

$BaTiO_3$ crystal precipitated in the crystallized samples.

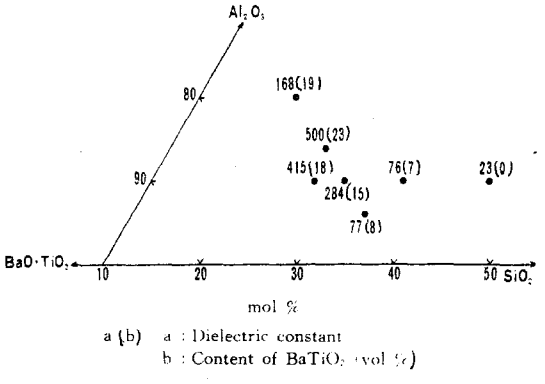

Fig. 1.7. Dielectric constant and content of $BaTiO_3$ crystal of the crystallized samples.

It is seen from Table 1.2. that the dielectric constant of the parent glass shows only slight dependence on the chemical composition, varying within the range from 14 to 18, wheares that of the crystallized glass is very much dependent on the chemical composition of the parent glass, varying from 23 to 500. Fig. 1.7 shows that with constant Al_2O_3 content the dielectric constant of the crystallized glass decreases as the $SiO_2/BaO \cdot TiO_2$ mole ratio increases and with constant $BaO \cdot TiO_2$ content the dielectric constant reaches a maximum when the Al_2O_3/SiO_2 mole ratio is 35/65.

3. Discussion

3.1. Dependence of Dielectric Constant on Chemical Composition

It was shown in the foregoing section that the dielectric constant of the crystallized glass is very much dependent on the chemical composition of the parent glass. This may be attributed to the dependence of the amount of $BaTiO_3$ crystal

precipitated in the crystallized glass on the chemical composition. The comparison of the dielectric constant with $BaTiO_3$ crystal content (Fig. 1.7) confirms that, in general, the dielectric constant increases with increasing volume fraction of $BaTiO_3$ crystal. The crystallized glass of the composition No. 1 (dielectric constant 168 and crystal content 19 in Fig. 1.7) exhibits a considerably low dielectric constant, however, in spite of relatively high content of $BaTiO_3$ crystal present: The reason for this rather exceptional case may be explained in terms of cracks present in the crystallized glass.

3.2. Microstructure of Crystallized Glass

The crystallized glasses in the present system are regarded as the mixture of a high dielectric constant phase consisting of $BaTiO_3$ crystals and a low dielectric constant phase consisting of residual glass and other crystals than $BaTiO_3$. In general, the dielectric constant of the mixture depends on the dielectric constant, volume fraction, shape and arrangement (regular or irregular) of the constituent phases and the type of mixing. Mixtures are divided into two classes by the type of mixing, one is "pure mixture" consisting of only particles and the other is "porphyritic mixture" in which particles are dispersed in another continuous phase.

Bruggeman[3] has derived relationship between the dielectric constant of the mixture (ε) and the volume fractions (δ_1 and δ_2) of the constituent phases for the following four cases.

(A) Three dimensional pure mixture of lamellar particles

irregularly dispersed:

$$\epsilon = 1/2(-\epsilon_\perp + \sqrt{\epsilon_\perp(8\epsilon_{//} + \epsilon_\perp)})$$

(B) Three dimensional pure mixture of spherical particles irregularly dispersed:

$$\epsilon = 1/4(2\epsilon_{//} - \epsilon'_{//} + \sqrt{(2\epsilon_{//} - \epsilon'_{//})^2 + 8\epsilon_1\epsilon_2})$$

(C) Three dimensional porphyritic mixture in which lamellar particles are irregularly dispersed in matrix:

$$\epsilon = \epsilon_1(3\epsilon_2 + 2\delta_1(\epsilon_1 - \epsilon_2))/(3\epsilon_1 - \delta_1(\epsilon_1 - \epsilon_2))$$

(D) Three dimensional porphyritic mixture in which spherical particles are irregularly dispersed in matrix:

$$1 - \delta_1 = (\epsilon_1 - \epsilon)(\epsilon_2/\epsilon)^{1/3}/(\epsilon_1 - \epsilon_2)$$

Here

$1/\epsilon_\perp = \delta_1/\epsilon_1 + \delta_2/\epsilon_2$,

$\epsilon_{//} = \delta_1\epsilon_1 + \delta_2\epsilon_2$,

$\epsilon'_{//} = \delta_1\epsilon_2 + \delta_2\epsilon_1$ and

ϵ_1 and ϵ_2 = dielectric constant of each constituent phases.

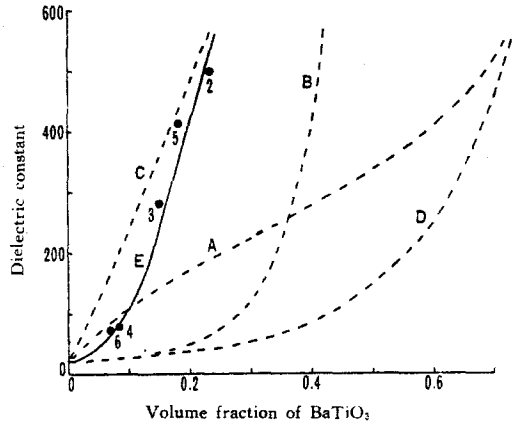

A : Pure mixture of lamellar particles
B : Pure mixture of spherical particles
C : Porphyritic mixture in which lamellar barium titanate crystals are dispersed in matrix
D : Porphyritic mixture in which spherical barium titanate crystals are dispersed in matrix
(A~D : Calculated from Bruggeman's equations)
E : The experimental results by authors

Fig. 1.8. Dielectric constant as a function of $BaTiO_3$ content.

Fig. 1.8 shows the dependences of dielectric constant of the mixture on volume fraction of $BaTiO_3$ calculated for the above four cases. In the calculation the dielectric constant of $BaTiO_3$ crystal was assumed 3300, a value which was obtained by extrapolating the measured dielectric constants of the crystallized glasses to the $BaTiO_3$ volume fraction of unity. The dielectric constant of the other phase was assumed 20, a value which is nearly equal to the dielectric constant of the parent glasses and their crystallized products containing no $BaTiO_3$ crystal. The solid circles in Fig. 1.8 represent the experimental data obtained on the crystallized glasses of the composition given in Table 1.1. The solid line was drawn so that it might fit best to the experimental data. It can be seen from the figure that the equation (C) describes the experimental results best. Therefore the crystallized glasses in this system are assumed to have the structure of porphyritic mixture in which lamellar barium titanate crystals with dielectric constant of 3300 are irregularly dispersed in matrix consisting of residual glass and crystal phases such as $BaAl_2Si_2O_8$ and $BaTiSiO_5$ with dielectric constant of 20. Deviation of experimental data from Bruggeman's relationship (C) at the region of low $BaTiO_3$ content may be attributed to the different size or shape of the $BaTiO_3$ crystals at low $BaTiO_3$ content from at high $BaTiO_3$ content. More detailed studies, however, are required for elucidating this matter.

Herczog[1] also investigated the relation between the dielectric constant of the crystallized glass and the volume fraction of constituent $BaTiO_3$ crystal for the glasses with

the composition $xBaTiO_3+(100-x)BaAl_2Si_2O_8$ (x by weight) and reported that the experimental data fits best to the relationship (B) for pure mixture of spherical particles, in contrast to the present results obeying the relationship (C). The reason for this is not known. Further study is required.

4. Summary

1. Glass formation region in the system $BaO \cdot TiO_2$-Al_2O_3-SiO_2 was determined and it was confirmed that the glasses containing higher amounts of BaO and TiO_2 components can be prepared in the present system containing Al_2O_3 than in the system $BaO \cdot TiO_2$-SiO_2.

2. Crystallization of the glasses in this system started at about 850°C and was essentially completed at about 1100°C. Crystals precipitated in the glasses heated to 1100°C were perovskite-type $BaTiO_3$, hexacelsian ($BaAl_2Si_2O_8$), $BaTiSiO_5$ and some unidentified crystals. Crystallized products obtained from the parent glasses containing too much amount of $BaO \cdot TiO_2$ or Al_2O_3 showed defects such as cracks and surface ripples.

3. Dielectric properties of the crystallized products varied with the composition of the parent glass. With constant Al_2O_3 content, the dielectric constant decreased with increasing $SiO_2/BaO \cdot TiO_2$ mole ratio. With constant $BaO \cdot TiO_2$ content, it reached a maximum when the Al_2O_3/SiO_2 mole ratio was 35/65. Generally, the dielectric constant increased with increasing amount of $BaTiO_3$ crystals precipitated in the crystallized products. The highest dielectric constant measured in the present experiments was 500 at a frequency

of 10^6c/s, that was obtained with the crystallized glass of the composition $BaO \cdot TiO_2$ 60, Al_2O_3 14, SiO_2 26 mole %.

4. The dielectric constant-$BaTiO_3$ volume fraction relationship of the crystallized glass agreeded best with a Bruggeman's theoretical formula obtained by assuming that crystallized glass has the structure of porphyritic mixture in which lamellar $BaTiO_3$ crystals are dispersed in matrix of residual glass and other crystals.

References

1) A. Herczog, J. Am. Ceram. Soc., 47 107 (1964)

2) H.D. Megaw, Trans. Faraday Soc., 42A 224 (1947)
G.W. Marks and L.A. Monson, Ind. Eng. Chem., 47 1611 (1955)

3) D.A.G. Bruggeman, Ann. d. Phy., 24 636 (1935)

Chapter 2. Preparation and Properties of the Thin Sheet Glass-Ceramics

In many cases high dielectric constant ceramics are used in the form of thin sheet when they are utilized as components of electronic devices. The present chapter deals with a method for preparing the $BaTiO_3$ glass-ceramics in the form of sheet less than 100μ thick. Dielectric properties and microstructures of such thin sheets are studied and compared with those of bulk glass-ceramics, thicker than 1mm, discussed in the previous chapter.

1. Experimental

1.1. Preparation of Thin Glass Sheet

Glasses having the compositions $(100-x-y)BaO\cdot TiO_2+xAl_2O_3+ySiO_2$ in mole % were melted. Since the glasses of this series, especially those rich in BaO and TiO_2, were extremely fluid above their liquidus temperatures, glass films as thin as 1 to 10μ were easily formed by hand blowing. The films obtained in this way were, however, too thin and, accordingly, too fragile for handling after they were crystallized.

To obtain the thin sheets having a sufficient mechanical strength efficiently, an apparatus was designed in which the molten glass was passed through between a pair of rotating cast iron drums being in contact with each other. The apparatus used is schematically shown in Fig. 2.1(a). About 50g of the batch mixtures were melted in a platinum-10% rhodium

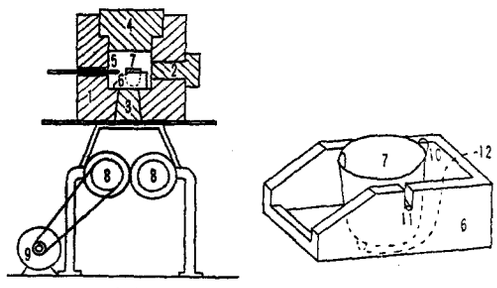

(a) (b)

1. Furnace, 2~4. Shutter, 5. Thermocouple, 6. Container for crucible, 7. Platinum-10% rhodium crucible, 8. Drum, 9. Moter, 10. Platinum wire, 11. Platinum arm, 12. Platinum wire

Fig. 2.1. Apparatus for preparing thin glass sheets.

crucible placed in an electric furnace with silicon carbide heating elements。 As shown in detail in Fig。 2.1(b), the crucible was suspended on two side-walls of an alumina refractory container by two platinum arms (sign 11) protruding from the outer surface of the crucible. After the glass batch was melted, the crucible was inclined by pulling a platinum wire (sign 12) welded at its end to the bottom of the crucible。 The molten glass was thus poured down drop by drop through a hole made in the bottom of the furnace, passed through between the two drums, 180mm in diameter, which rotated in mutual contact at a speed of 200 r.p.m, and finally issued in pieces in the form of leaf, about 50 mm^2 in area and about 50 to 100μ in thickness。 No sheet less than 50μ thick was obtained. Although the homogeneity in thickness of each piece of sheet was found to be much affected by the smoothness of the drum surface, it was not difficult technically to keep the variation of its thickness within $\pm$1μ.

1.2. Crystallization of Glass Sheets

The glass sheets thus prepared were placed on a square piece of platinum sheet and heated in the electric furnace with silicon carbide heating elements up to 1100°C at a rate of 5°C/min, then held at 1100°C for one hour followed by natural cooling in the furnace. The crystallized glass sheets were strong enough to withstand fairly rough handling.

1.3. Glass Formation Region

Various glasses of the composition corresponding to $(100-x-y)BaO\cdot TiO_2+xAl_2O_3+ySiO_2$ in mole % were melted at 1550°C and formed into piece of thin sheet by the method described above. The batch materials used were the same as in Chapter 1. Some of the sheets issuing from the drums devitrified partially or almost entirely, while others were transparent and glassy. A solid line in Fig. 2.2 represents the boundary between the two region, i.e. glass formation and devitrification regions. The dotted line in the figure

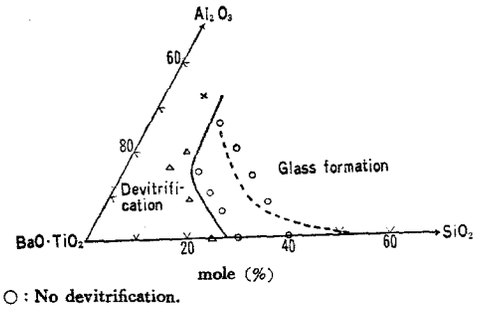

○ : No devitrification.
△ : Partial devitrification.
× : Extreme devitrification.
— : The limit of glass formation for preparation of film about 100 μ thick.
··· : The limit of glass formation for preparation of plate about 2 mm thick.

Fig. 2.2. Glass formation region in the system $BaO\cdot TiO_2$-Al_2O_3-SiO_2.

is the boundary given in Chapter 1 for the 2mm thick plate samples. It is seen that much broader glass formation region is obtained when the melts are formed into thin sheets. This is naturally because thin sheets are quenched with much higher rate.

1.4. Dielectric Properties

1.4.1. Dependence of Dielectric Properties upon Heat-Treatment

The glass sheets about 100μ thick of the composition No. 7 in Table 2.1 were subjected to various heat-treatments. Some samples were heated up to 900°, 1000°, 1100° and 1200°C, respectively, at a rate of 5°C/min and then allowed to cool outside of the furnace. The other samples were all heated up to 1100°C at a rate of 5°C/min, maintained at 1100°C for 0, 1, 3, 5 and 20 hours, respectively, and then cooled in the furnace.

Results of measurements on dielectric properties of the resultant crystallized glasses are shown in Fig. 2.3 and 2.4. Measurements of the dielectric constant and loss tangent were made by using a Q-meter (Type GM-102, Yokogawa Electric Works, Ltd.) at 1Mc/s at room temperature. Silver paint applied on both surfaces of the sample served as electrode.

1.4.2. Dependence of Dielectric Properties upon Composition

The glass sheets of the various compositions given in Table 2.1 were heated up to 1100°C at a rate of 5°C/min, maintained at 1100°C for 5 hours and then allowed to cool naturally in the furnace. The dielectric properties of the sheets thus obtained are shown in the composition triangle of Fig. 2.5. From the figure it is seen that the dielectric constant increases with increasing $BaO \cdot TiO_2$ content if the

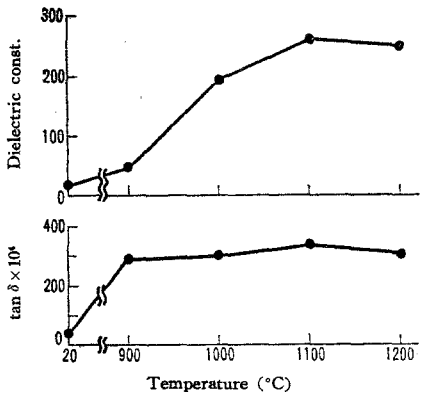

Fig. 2.3. Dependence of the dielectric properties of 100μ thick glass-ceramic sheet on heating temperature. Glass composition; No. 7.

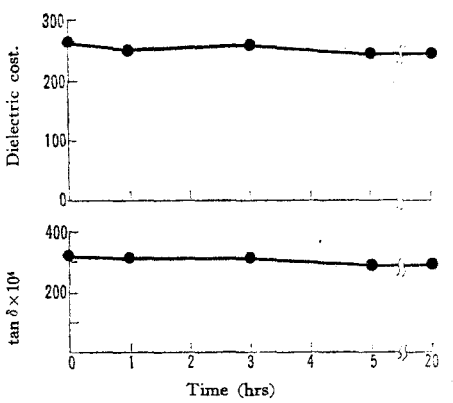

Fig. 2.4. Dependence of the dielectric properties of 100μ thick glass-ceramic sheet on heating time at 1100°C. Glass composition; No. 7.

mole ratio of Al_2O_3 to SiO_2 is the same and that a maximum value of dielectric constant is obtained at the mole ratio of Al_2O_3 to SiO_2 equaling about 35/65 for the same $BaO \cdot TiO_2$ content.

1.4.3. Dependence of Dielectric Properties on Sample Thickness

It was reported in Chapter 1 that the crystallized glass of the composition $BaO \cdot TiO_2$ 60, Al_2O_3 14 and SiO_2 26 by mole %,

Table 2.1. Glass composition

Sample No.	Composition (mole %) $BaO \cdot TiO_2$	Al_2O_3	SiO_2
1	70.0	15.0	15.0
2	70.0	10.5	19.5
3	70.0	6.0	24.0
4	70.0	0.0	30.0
5	60.0	26.0	14.0
6	60.0	20.0	20.0
7	60.0	14.0	26.0
8	60.0	8.0	32.0
9	60.0	0.0	40.0

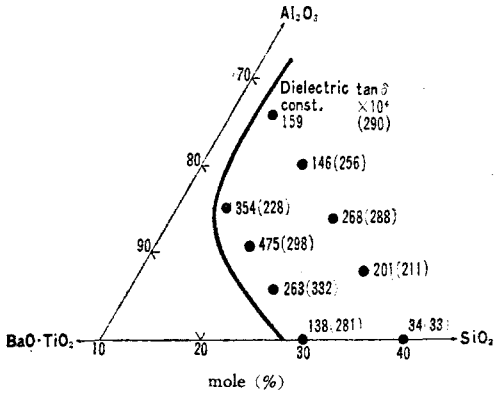

Fig. 2.5. Dielectric properties of 100μ thick glass-ceramic sheets obtained from $BaO \cdot TiO_2$-Al_2O_3-SiO_2 glasses.

when formed into the plate about 1mm thick, show a dielectric constant of about 500. This value is about twice of that (270) obtained for the 100μ thick thin sheet of the same composition (No. 7 in Table 2.1). In order to investigate the cause for this discrepancy the relation between the

dielectric constant and the sample thickness was examined in more detail using the samples of varying thickness for the composition $BaO \cdot TiO_2$ 60, Al_2O_3 14 and SiO_2 26 mole %. Samples of plate thicker than 100μ were prepared by pouring the glass melts on a steel plate and pressing with another piece of steel plate. Samples of sheet thinner than 100μ were obtained by the method described above. The thickness of the samples could be varied by changing the rate of rotation of the drums in the range between 20 and 300 r.p.m. The heat treatment applied was the same as described in the paragraph 1.2.

The results are shown in Fig. 2.6. It should be noted that the dielectric constant changes abruptly at the thickness of the sample of about 200μ.

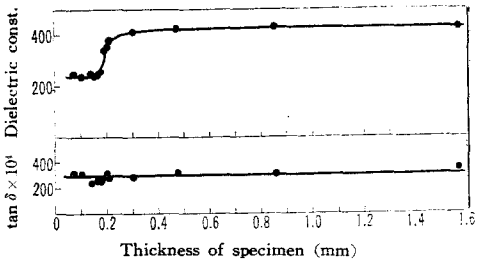

Fig. 2.6. Variation of the dielectric properties of glass-ceramics with thickness of the sample. Glass composition; No. 7.

1.5. Microstructure near the Surface

For reasoning the difference in dielectric constant between thin and thick samples, microstructure of the two crystallized samples (No. 7 in Table 2.1) having the thickness of 100μ and 1500μ was investigated. For convenience

the thinner sample will be refered to as the "sheet" and the thicker one the "plate" in the followings.

1.5.1. X-Ray Diffraction Analysis

First, the "sheet" and the "plate" were powdered and subjected to X-ray diffraction analysis. In both samples perovskite-type barium titanate ($BaTiO_3$) and hexacelsian ($BaAl_2Si_2O_8$) were identified. No differences in the position and intensity of their diffraction lines were observed between the both samples.

Secondly, in order to investigate the microstructure near the surface, the "plate" was successively ground to various depths by Al_2O_3 abrasive powder and, instead of powder form, the sample was mounted on a holder of X-ray diffractometer. The results of the X-ray analysis made of surfaces obtained by grinding are plotted against the depth from the original surface in Fig. 2.7. The figure

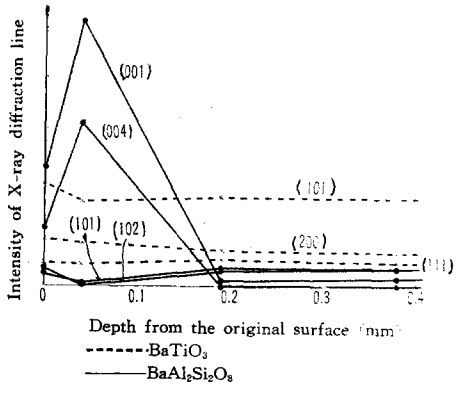

Fig. 2.7. Intensities of X-ray diffraction lines for the surfaces of the glass-ceramics ground to varying depths. Glass composition; No. 7.

shows that the intensities of the (101), (200) and (111) reflections of barium titanate and also those of the (101) and (102) reflections of hexacelsian are almost the same for all the ground surfaces irrespective of their depth from the original surface. In marked contrast to these, the intensities of the (001) and (004) reflections of hexacelsian show great changes with the depth from the original surface; they are markedly great for the surfaces from the origianl surface to the depth of 100μ, but reach the respective constant values at the depths over about 200μ.

The relative intensity among the three lines for barium titanate and also among the four lines for hexacelsian, for the ground surface deeper than 200μ, was found to be the same, respectively, as those determined for the powdered "plate" samples described above.

Although changes in intensities of the X-ray diffraction lines with the depth removed were not investigated for the "sheet" samples because of the technical difficulty of their successive grinding, the X-ray diffraction chart obtained only for the original surface of the "sheet" was the same as that of the "plate".

1.5.2. Observation with Metallurgical Microscope

Fig. 2.8 is a reflection micrograph of a polished cross-section of a piece of "plate". A rim of about 200μ in width exhibits a texture different from that of the interior. Such a rim, however, was not always observed on all of the cross-sections, although the presence of a rim with peculiar structure was indicated by the X-ray

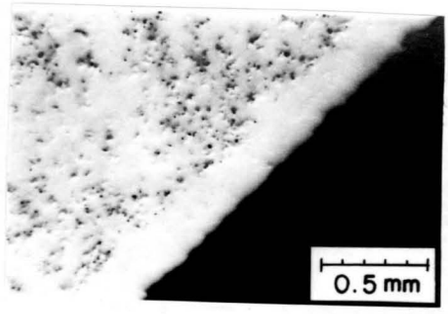

Fig. 2.8. Cross-section of glass-ceramics (No. 7)

diffraction analysis. In other words the observation with the metallurgical microscope can not be always relied upon for the confirmation of the presence of a special microstructure near the surface of the "plate", although it is a simple and useful method for the morphological investigation of the microstructure.

1.5.3. Observation with Electron Microscope

Electron microscopic examination was made of the original surfaces of the "plate" and the "sheet". Also the surfaces of the "plate" ground away by 40μ and 400μ in depth from their original surfaces were examined. All of the surfaces were etched by immersing the samples in 5 % NaOH at 50°C for 75 min and their chromium-shadowed carbon replicas were prepared.

Fig. 2.9(a) through (d) are the electronmicrographs of their respective surfaces. No marked difference is found in appearence between Fig. 2.9(a) and (b). In Fig. 2.9(c) two kinds of crystal particles, i.e. spherical particles of 0.2 to 0.7μ in diameter and acicular particles of 0.05 to 0.5μ in width and 0.5 to 3μ in length, are observed. Judging from their crystal habits, majority of the spherical ones are barium titanate and the acicular ones

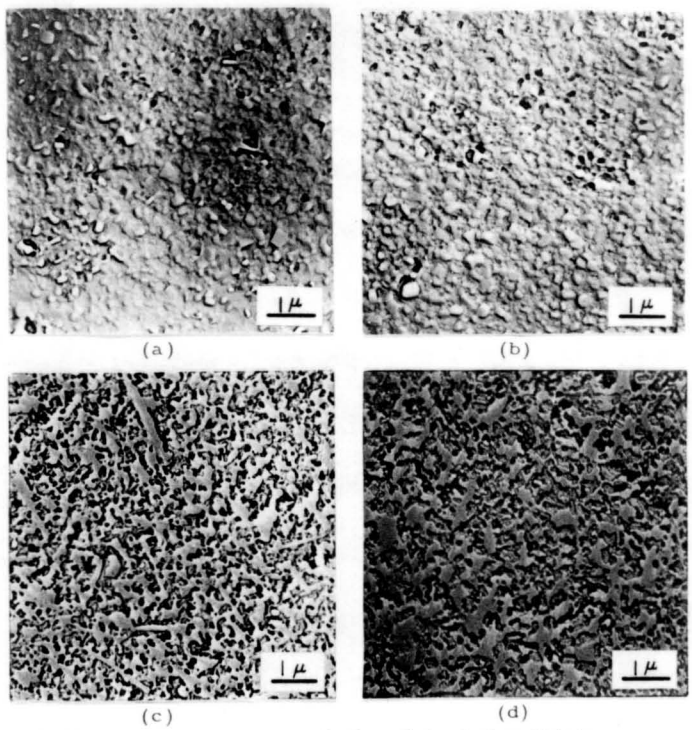

(a) The original surface of the plate 1.5mm thick.
(b) The original surface of the sheet 100μ thick.
(c) The surface of the plate ground to a depth of 40μ.
(d) The surface of the plate ground to a depth of 400μ.

Fig. 2.9. Electron micrographs of glass-ceramics No. 7.

hexacelsian with an orientation parallel to the surface of the samples. No essential difference is found in appearence between Fig. 2.9(c) and (d), except that the number of the crystals with acicular morphology appears to be larger for Fig. 2.9(c) than (d).

2. Discussion

Decrease in dielectric constant with decreasing thickness of the samples is an adverse effect, especially when the $BaTiO_3$ glass-ceramics are used as capacitors in the electric circuit.

In general, the dielectric constant of the polyphase material containing a ferroelectric phase is determined by

the kind, size, volume fraction and arrangement of the constituent phases. The results of the X-ray diffraction analysis made for the powdered samples indicated that there is no difference in position and intensity of all the diffraction lines between the "sheet" and "plate". This means that in both samples the kinds of crystals separated out and also their respective amounts are the same. No difference was indicated in the size of the crystals separated out by the electron microscopic examination between the original surfaces of the "plate" and "sheet".

The only factor left to be considered on discussing the dielectric constant of the present polyphase material (glass-ceramic sheet) is, therefore, the arrangemant of the constituent crystals. Concerning the arrangement of the crystals, the following characteristic feature confirmed by the X-ray diffraction analysis for the "plate" sample would serve as a basis for the discussion. It was indicated that for hexacelsian crystals precipitating near the original surface of the sample the intensities of the (001) and (004) reflections were quite large while those of the (101) and (102) reflectins were slightly small, both compared with diffraction lines of hexacelsian in the interior of the sample. This can be interpreted as a result of preferred orientation of the hexacelsian at the surface. Generally, hexacelsians are likely to separate out as lath-like crystals with cleavage parallel to their (001) plane[1]. Near the surface of the "plate" samples hexacelsian probably appear in such a manner that their cleavage planes are parallel to the surface of the samples. The crystals with the

acicular morphology observed with electron microscope very near the original surface of the "plate" samples (Fig. 2.9 (c)) would thus be the hexacelsian having such a preferred orientation. In the interior of the "plate" samples, i.e. the portion deeper than 200μ, hexacelsian would distribute rather at random without preferred orientation, as evidenced from that the relative intensities of the X-ray diffraction lines of hexacelsian present in the portion deeper than 200μ are equivalent to those of the powdered sample. This is also supported by the electron microscopic observation that the number of the acicular crystals of the two portions near and far apart from the original surface are different.

The dielectric constant of hexacelsian itself would be by far the lower than those of the mixture of barium titanate and their surrounding glass matrix. Thus the portion near the surface of the "plate" is considered to have a structure in which high-capacitive elements consisting of barium titanate and the glass matrix, and low-capacitive elements consisting of hexacelsian with a preferred orientation are connected in series. Consequently the dielectric constant of this surface layer would be much lower than that of the interior in which the hexacelsian are precipitated without preferred orientation[2].

When the sample is thick, an effect of the surface layer with low capacity is insignificant on the apparent dielectric constant of the whole sample. With decreasing the thickness, especially when it reachs about 200μ, however, the effect would be strong enough to cause a sudden decrease in dielectric constant of the sample.

Orientation of the hexacelsian in the "sheet" sample was unfortunately unable to be confirmed because of the experimental difficulties. It seems, however, to be natural to consider that the "sheet" sample has the similar structure to that of portion near the origianl surface of the "plate" sample having the hexacelsian with a preferred orientation.

The lower value in dielectric constant of the "sheet" than that of the "plate" would thus be explained.

3. Summary

1. Glass-ceramic thin sheets of 50 to 100μ in thickness having dielectric constant of 500 and tanδ of 0.03 (at 10^6c/s) at the optimum conditions were prepared from glasses of the system $BaO \cdot TiO_2$-Al_2O_3-SiO_2 by a method which comprises sqeezing the glass melts by the two drums of solid cast iron rotating in mutual contact and subjecting the produced glass sheets to heat treatments.

2. It was found that the dielectric constant of the glass-ceramics of this type is reduced to a half of that of their bulk when formed into a sheet thinner than about 200μ. Its cause was attributed to a preferred orientation of hexacelsian precipitated near the surface of the sample.

References

1) B. Yoshiki and K. Matsumoto, Res. Rep. Asahi Glass Co., 1 (1) 8(1950).

2) W.D. Kingery, Introduction to Ceramics, John Wiley & Sons. Inc., p.719 (1960).

Chapter 3. Crystallization Process of the $BaO \cdot TiO_2$-Al_2O_3-SiO_2 Glass

In Chapter 2, it was shown that the dielectric constant of BaO-TiO_2-Al_2O_3-SiO_2 glass-ceramics decreases with decreasing thickness of the sample and its cause was attributed to the presence of the hexacelsian crystals ($BaAl_2Si_2O_8$) at the surface of the sample, which are oriented preferentially with their cleavage planes (001) parallel to the surface of the sample.

The main objective of the present investigation is to find the cause of the preferred orientation of the hexacelsian crystals. For this purpose, the crystallization process of the $BaO \cdot TiO_2$-Al_2O_3-SiO_2 glass at the surface of the sample as well as in its interior was investigated by X-ray diffraction analysis, electron microprobe analysis and optical microscopic technique.

1. Experimental

1.1. Glass Preparation

The glass of the composition $BaO \cdot TiO_2$ 60, Al_2O_3 14 and SiO_2 26 mole % was used. The dielectric properties and microstructure of the glass-ceramics of this composition were already reported in Chapter 2. The batch materials used were the same as in Chapter 1. The batches were melted at 1450°C in platinum-10% rhodium crucibles. The melts were poured on a steel plate, formed into 3mm thick plates and

annealed at 650°C. Rectangular pieces, 10 by 10 by 2mm were cut from the plates, ground and subjected to the following experiments.

1.2. Analysis of Crystallization Process

1.2.1. X-ray Diffraction Analysis

The glass sample were placed on a platinum sheet and heated in a silicon carbide electric furnace up to various temperatures in the range from 700° to 1100°C, respectively at a rate of 5°C/min and , after the respective temperature was reached, allowed to cool outside of the furnace. X-ray diffraction analyses were made of their virgin (original) surfaces as well as those ground to a depth of about 700μ by turning X-ray beam (nickel-filtered Cu-Kα) directly on their surfaces.

No difference was found in X-ray diffraction patterns for the two virgin surfaces; the one having faced the platinum sheet during the heat treatment and the opposite surface. However, great differences were found between the virgin surface and ground surface. The X-ray diffraction patterns for the virgin and ground surface of the sample heated to 850°C are given in Fig. 3.1. The characteristic X-ray diffraction peaks for the interior of the sample corresponded to those for the barium titanate ($BaTiO_3$) and hexacelsian ($BaAl_2Si_2O_8$) crystals given in an ASTM powder diffraction file, whereas the peaks for the virgin surface did not correspond to any pattern found in the file.

Relations between the intensity of the highest diffraction peak for each of the crystals and the temperature of heat treatment of the samples in which the crystals precipitated are shown in Fig. 3.2(a) and (b), respectively, for

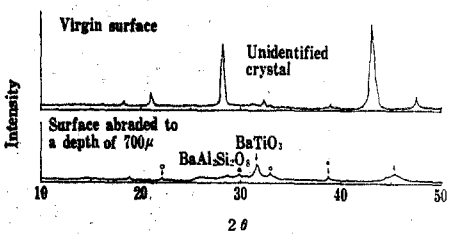

Fig 3.1. X-ray diffraction pattern for the sample heated to 850°C.

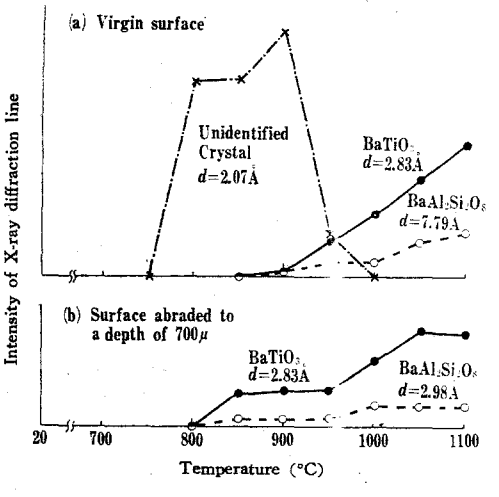

Fig. 3.2. Change in intensities of X-ray diffraction lines obtained for the glasses heated to various temperatures.

the virgin surface and the ground surface of the samples. Comparison of the two figures shows that there is a great difference in crystallization process between the virgin surface and the interior. At the virgin surface, the unidentified crystal as described above starts to precipitate at 750°C, and the $BaTiO_3$ and $BaAl_2Si_2O_8$ crystals start to precipitate at 850°C at the expence of the unidentified

crystal. In the interior, however, the unidentified crystal does not precipitate and the $BaTiO_3$ and $BaAl_2Si_2O_8$ crystals start to precipitate at the temperature as low as 800°C. It should be noted that the highest X-ray diffraction peak is different for the $BaAl_2Si_2O_8$ crystals precipitated at the virgin surface and in the interior; the peak at d=7.79Å is the highest for the former, while the peak at 2.98Å is the highest for the latter. This would suggest a preferred orientation of the crystals precipitated at the virgin surface.

Although the above description is concerned with the results for the samples, the surface of which had been ground before the heat treatment, the same results were obtained for the as-cast glass not ground.

1.2.2. Optical Microscopic Analysis

The glass samples heat-treated at various temperatures as described in the previous section were sawed perpendicular to their virgin surfaces to prepare their thin sections about 0.03mm thick. In Fig. 3.3 are shown their photographs taken with a polarizing microscope with crossed nicols. In the sample heated to 800°C a 30μ thick layer consisting of numerous needle-like crystals grown from the virgin surface is observed. In the sample heated to 950°C the thickness of the layer reaches 200μ. Besides the growth of the needle-like crystals the formation of crystal particles less than 1μ in diameter is observed in the interior of the sample heated to 900°C. For the two samples heated to 1000° and 1100°C, respectively, disappearence of the needle-like crystals and spread of the region of the small crystal

particles toward the virgin surface of the samples are observed.

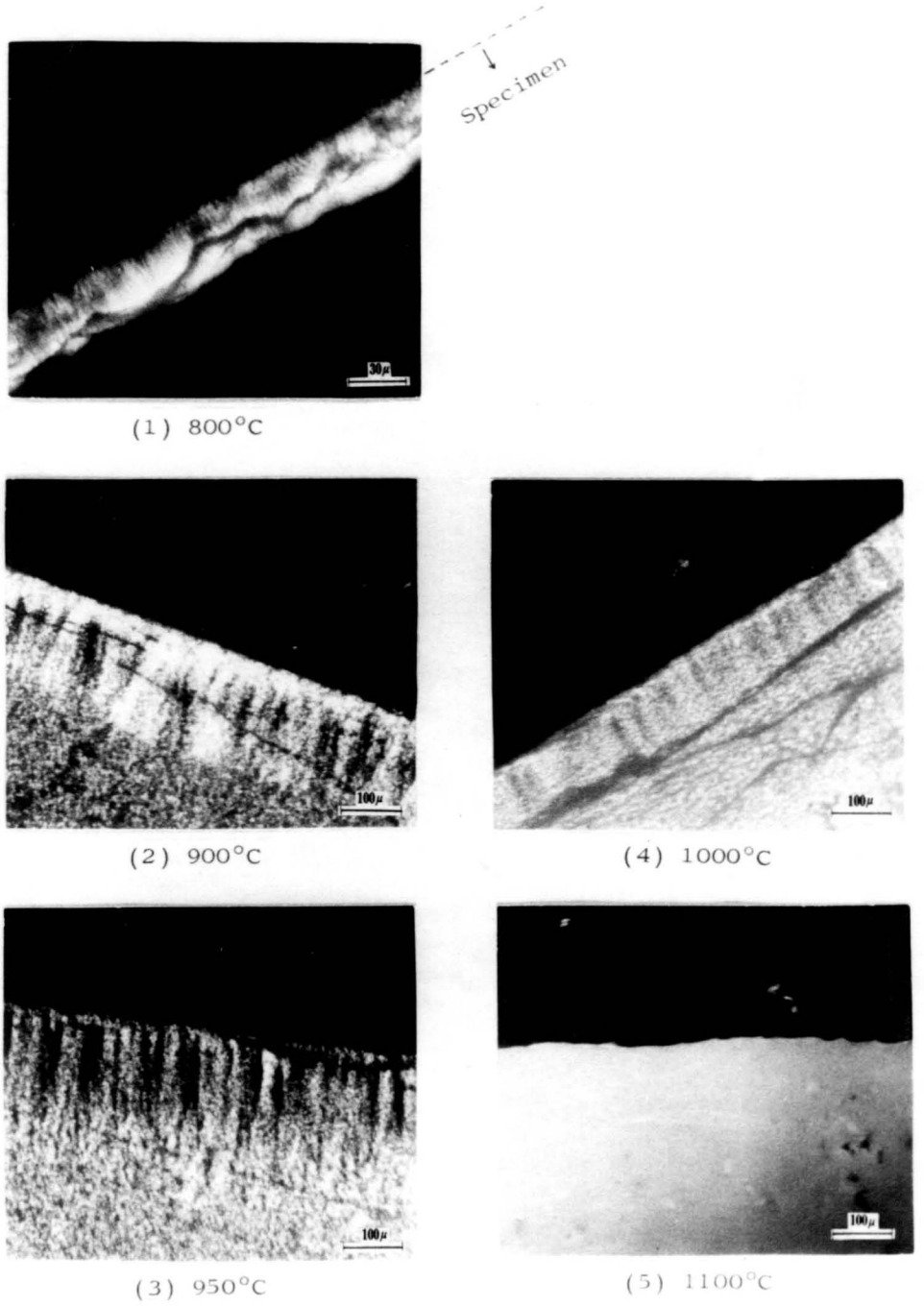

Fig. 3.3. Cross-sections of the samples heated to various temperatures (crossed nicols).

1.3. Properties of the Crystals Precipitated Intermediately in the Course of Heat Treatment

1.3.1. Chemical Composition

The needle-like crystals observed under the optical microscope are considered to correspond to the "unidentified" crystals in the X-ray diffraction analysis which appeared intermediately in the course of heat treatment. In order to determine their chemical composition, the glass sample heated to 800°C (vid. Fig. 3.3(1)) was cut along the direction perpendicular to its virgin surface, and the resultant cross-section, after polished with chromium oxide powders and covered with a thin conductive layer of vacuum-deposited carbon, was examined by an electron microprobe X-ray analyzer (Shimazu ARL) with a 2μ-diameter X-ray spot, 20kV accelerating voltage and 0.1μA beam current.

Fig. 3.4. shows the variations of X-ray intensities of Ba, Ti, Al and Si obtained when the cross-section was scanned by the electron beam along the direction perpendicular to the virgin surface of the sample and also when scanned in the direction parallel to the virgin surface at the position 10μ apart from it. In either case the electron beam might have crossed over a boundary between the unidentified needle-like crystals and the region as yet glassy. However, no appreciable difference in X-ray intensity was observed between the above two regions, suggesting that the compositions of the unidentified crystal and the glass from which it grew are almost the same.

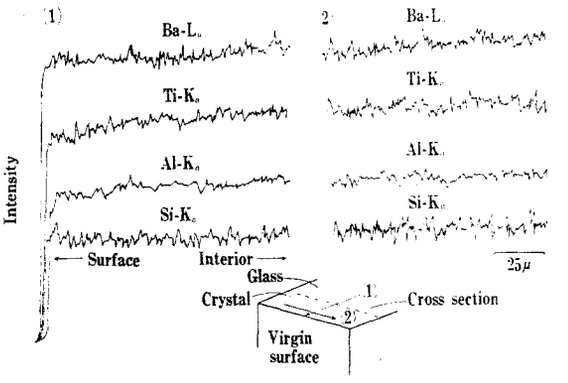

Fig. 3.4. EMX for the glass of which surface was crystallized.

1.3.2. Structure

It is quite probable that the X-ray diffraction pattern given in Fig. 3.1 has been affected by the intrinsic preferred orientation of the crystals since it was obtained by exposing the surface of the sample to the X-ray beam. This effect must be avoided to studying the crystal structure. For this purpose the glass sample was powdered to -100 mesh, heated to 800°C on a platinum sheet, allowed to cool outside of the furnace and reground to -200 mesh.

The X-ray diffraction pattern obtained for this powdered sample is shown in the upper part of Fig. 3.5, which shows a great resemblance to that of the hexagonal benitoite ($BaTiSi_3O_9$) type given in the tabulated diffraction data by L.K. Frevel et al.[1] The lower part of Fig. 3.5 shows a pattern for the benitoite-type crystal with the cell dimensions of a=5.50 and c=8.34Å. The cell dimensions of the natural benitoite crystal ($BaTiSi_3O_9$) reported by W.H. Zachariasen are a=6.60 and c=9.71Å.

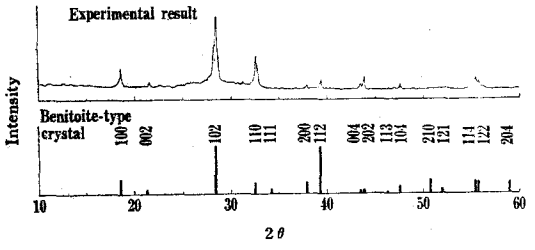

Fig. 3.5. X-ray diffraction pattern for the powdered sample heated to 800°C (top) and that for hexagonal benitoite-type crystal with the cell dimensions of a=5.50Å and c=8.34Å (bottom).

1.3.3. Stability of the Intermediate Crystal

The glass sample in the form of plate was heated to 800°C at a rate of 5°C/min, maintained at 800°C for various lengths of time and allowed to cool in air. The X-ray diffraction analysis was made of the sample thus heat-treated by exposing its surface to the X-ray beam. Fig. 3.6 shows the intensity variation of diffraction lines of the intermediate crystal (the benitoite-type), $BaTiO_3$ and hexacelsian with the heating period.

The figure shows that the amount of the intermediate crystal decreases, whereas those of the $BaTiO_3$ and hexacelsian increase with increasing heating period. This indicates that at 800°C the intermediate crystal is metastable, and the barium titanate and hexacelsian are stable.

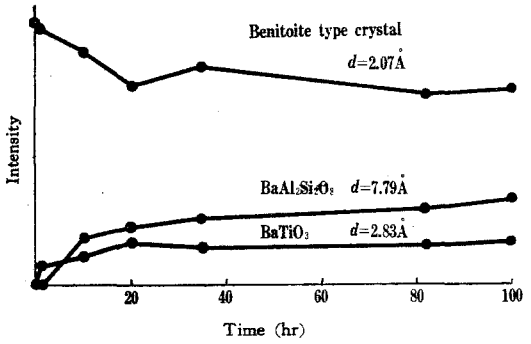

Fig. 3.6. Dependence of the intensities of X-ray diffraction lines on the heating period at 800°C.

2. Discussion

The orientation of the hexacelsian crystal in the $BaO \cdot TiO_2$-Al_2O_3-SiO_2 glass-ceramics made by the heat treatment at 1100°C is shown in Fig. 3.7, which is the schematic representation of the description in Chapter 2. Difference in orientation between the hexacelsian crystals precipitated near the surface and in the interior of the sample may be explained as follows.

Fig. 3.7. Arrangement of the hexacelsian crystals in the glass-ceramics.

In the interior of the glass sample, the $BaTiO_3$ and hexacelsian crystals are nucleated homogeneously and grow in size without any particular orientation, since there is no pre-existing surface. Their growth proceeds without

any transformation up to 1100°C. The random arrangement of the hexacelsians in the interior of the sample may thus be explained.

Near the surface of the glass sample, however, the metastable benitoite-type crystals precipitate first and then progressively transform to the $BaTiO_3$ and hexacelsian as the temperature is raised. The benitoite crystal, as shown in Fig. 3.8, has a layered structure[2], in which layers consisting of Si_3O_9 rings are arranged parallel to (001) plane and barium and titanium ions exist between these layers. The metastable crystal found in the present experiment is considered to have a structure similar to that of the benitoite crystals. Also hexacelsian crystal, as shown in Fig. 3.8, has a layered structure[3], in which layers having the composition $((Si,Al)O_2)_n$ are parallel to (001) plane and barium ions exist between these layers.

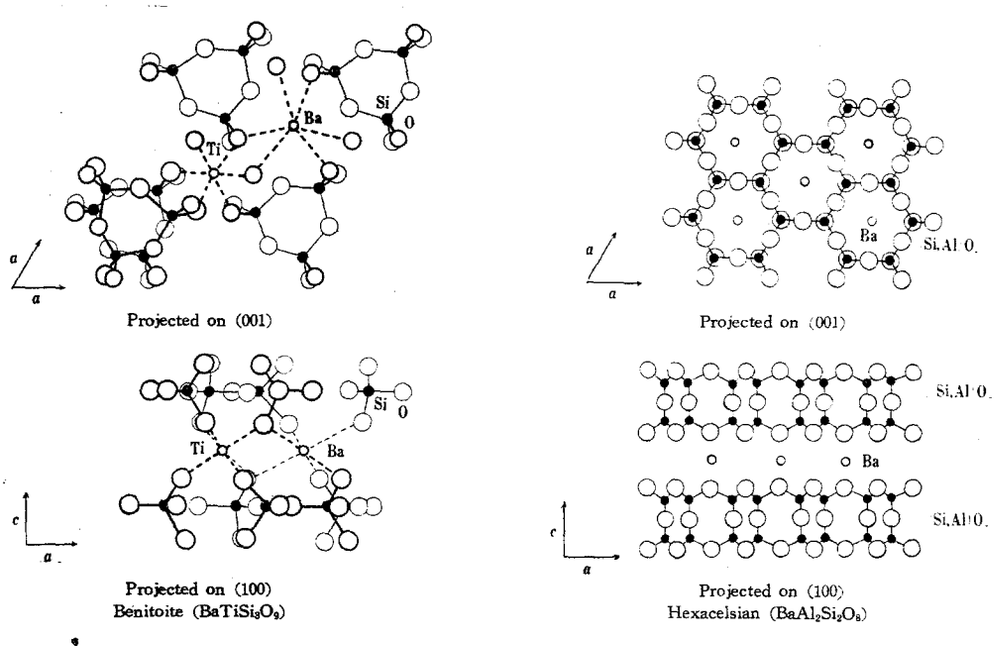

Fig. 3.8. The structures of benitoite and hexacelsian.

Since both the metastable benitoite-type crystal and hexacelsian have the layered structure characterized by the silicate layer parallel to (001) plane, the hexacelsian crystals, when formed from the metastable benitoite-type crystal, will orient itself in the manner that the direction of its silicate layer will be the same as that of the silicate layer in the metastable crystal. Furthermore, (004) X-ray reflection of the metastable benitoite-type crystal (Fig. 3.1) formed on the surface of the glass sample is extraordinarily stronger than the reflection for the powdered glass (Fig. 3.5), indicating that the (001) plane of the metastable benitoite-type crystal is parallel to the surface of the glass sample. The preferred orientation of the hexacelsian crystals near the surface of the glass sample is thus attributed to the preferred orientation of the mother crystals of metastable benitoite-type from which the hexacelsian was formed. The process whereby the hexacelsian precipitated near the surface of the glass is shown schematically in Fig. 3.9.

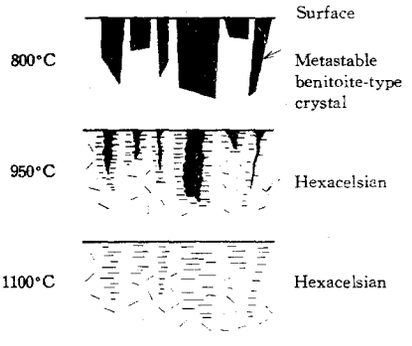

Fig. 3.9. Crystallization of hexacelsian near the surface of the glass.

The $BaTiO_3$ crystals did not show any preferred orientation whether near the surface or in the interior of the glass, though they were also formed from the mestastable benitoite-type crystals. This is attributed to the lack of resemblance in structure between the $BaTiO_3$ and benitoite-type crystal.

The reason why the metastable crystals of benitoite-type are formed only near the surface of the glass sample remains unexplained. Since compositional difference was not detected between near the surface and in the interior of the glass by electron microprobe analysis, it seems unlikely that the metastable phase was caused by the compositional difference between the surface and in the interior. It also can not be attributed to the surface contamination because both the virgin surface of the as-cast glass and the pre-ground surface showed the same results. Some other reason, for example, the difference in valency or coordination number of the constituting ions between at the surface and in the interior of the glass sample, should be considered.

3. Summary

1. Crystallization process of the $BaO \cdot TiO_2$ 60, Al_2O_3 14, SiO_2 26 mole % glass was examined in detail, with a particular attention to the difference between surface and in the interior. It was found that near the surface of the glass, a metastable benitoite-type crystal was formed first and then transformed progressively to the stable $BaTiO_3$ and hexacelsian whereas in the interior the $BaTiO_3$ and hexacelsian were formed originally.

2. The cause of the preferred orientation of hexacelsian in the crystallized products was attributed to the preferred orientation of the metastable benitoite-type crystal and the resemblance of the structure between the benitoite-type crystal and hexacelsian.

References

1) L.K. Frevel and H.W. Rinn, Anal. Chem., 25 1697 (1953).

2) W.H. Zachariasen, Zeits. Krist., 74 139 (1930).
L. Bragg and G.F. Claringbull, Crystal Structures of Minerals, G. Bell and Sons, Ltd., p. 212 (1965).

3) B. Yoshiki and K. Matsumoto, Res. Rep. Asahi Glass Co., 1 8 (1950).

PART II. GLASS-CERAMICS IN THE SYSTEM $PbO\text{-}TiO_2\text{-}Al_2O_3\text{-}SiO_2$

Chapter 4. Preparation and Properties of the Bulk Glass-Ceramics

Lead titanate ($PbTiO_3$) ceramics have not been obtained by the conventional method of sintering crystalline powders because of the anisotropic and extraordinarily large expansion of the constituent crystals at their transition temperature. Nevertheless, $PbTiO_3$ is paid attention to as one of the promising materials for capacitors because of its high Curie point (490°C) resulting in a small and linear temperature dependence of its dielectric constant up to fairly high temperatures. Furthermore, it can be expected that glasses containing a large amount of PbO are crystallized at relatively low temperatures. This behavior is advantageous for producing glass-ceramics and metal composites such as capacitors because electrodes of silver and copper applied to glass articles are not adversly affected during their crystallization.

This chapter deals with the glass formation in the system $PbO\text{-}TiO_2\text{-}Al_2O_3\text{-}SiO_2$, crystallization of the glass in this system, dielectric properties of the crystallized products in relation to their microstructures.

Stookey[1] reported that homogeneous glass-ceramics consisting of crystallites of perovskite-type lead titanate

($PbTiO_3$) can be obtained from a glass in the system described above. Russell et al.[2)3)] established later that its crystallization proceeds via its glassy two-phase separation. Bergeron et al.[4)] investigated the growth rate of $PbTiO_3$ crystals from a $PbO-B_2O_3-TiO_2$ glass. Martin[5)] found that on heating $PbO-TiO_2-SiO_2-B_2O_3$(or Na_2O) glasses a metastable pyrochlore-type lead titanate precipitates first and by further heating it transforms to the perovskite-type $PbTiO_3$. Grossman et al.[6)] presented a brief report on the dielectric properties of $PbO-TiO_2-BaO-B_2O_3$ glass-ceramics. Effects of the chemical composition of glasses on their crystallization and on dielectric properties of their crystallized products, however, have not yet been studied systematically.

1. Experimantal

1.1. Glass Formation Region

For determination of the glass formation region in the system $PbO-TiO_2-Al_2O_3-SiO_2$, glasses of the compositions given in Table 4.1 were melted. The batch materials used were red lead, titanium oxide and aluminum hydroxide, all of cp-grade, and pure quartz powders for manufacturing optical glasses. About 150g of the mixed batch materials were put in a platinum-10% rhodium crucible of 50cc in capacity, covered with a lid, and melted in a SiC furnace at 1400°C for 1 hour. The melts were poured on a steel plate and pressed into the form of plate approximately 3mm thick. They were reheated at 400°C in a furnace for annealing.

Their glass formation tendencies examined by the naked eye are given in the right column of Table 4.1. They are

Table 4.1. Compositions investigated and their glass formation tendency

Sample No.	Composition (mole %) PbO	TiO_2	Al_2O_3	SiO_2	Glass formation tendency*
1	52.0	23.0		25.0	x
2	43.1	26.9		30.0	Δ
3	48.0	22.0		30.0	Δ
4	32.5	32.5		35.0	x
5	40.0	25.0		35.0	o
6	45.0	20.0		35.0	o
7	50.0	15.0		35.0	Δ
8	27.5	27.5		45.0	x
9	33.8	21.2		45.0	o
10	38.0	17.0		45.0	o
11	43.1	26.9	4.3	25.7	Δ
12	40.0	25.0	5.0	30.0	o
13	45.0	20.0	5.0	30.0	o
14	33.8	21.2	6.4	38.6	o
15	38.0	17.0	6.4	38.6	o
16	43.1	26.9	8.6	21.4	x
17	48.5	21.5	8.6	21.4	Δ
18	32.5	32.5	10.0	25.0	Δ
19	40.0	25.0	10.0	25.0	o
20	45.0	20.0	10.0	25.0	o
21	27.5	27.5	12.9	32.1	x
22	33.8	21.2	12.9	32.1	o
23	38.0	17.0	12.9	32.1	o
24	43.1	26.9	13.0	17.0	Δ
25	48.0	22.0	13.0	17.0	x
26	32.5	32.5	15.0	20.0	x
27	40.0	25.0	15.0	20.0	o
28	45.0	20.0	15.0	20.0	o
29	33.8	21.2	19.3	25.7	Δ
30	38.0	17.0	19.3	25.7	o
31	40.0	25.0	20.0	15.0	Δ
32	45.0	20.0	20.0	15.0	Δ
33	33.8	21.2	25.7	19.3	x
34	38.2	16.8	25.7	19.3	x

* o ; No devitrification
Δ ; Partial devitrification
x ; Extreme devitrification

also summarized in a composition triangle in Fig. 4.1. The three solid curves indicate the boundaries between the regions of transparent glass formation and devitrification for the groups of compositions having the R values of 0, 2/5 and 3/4, respectively.

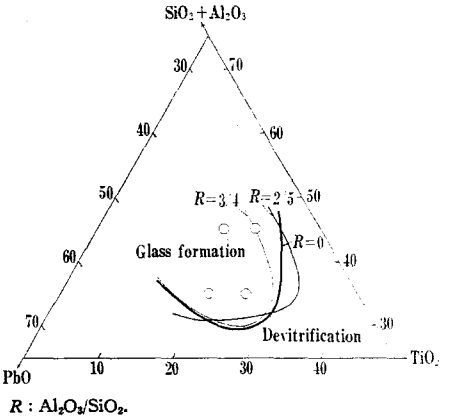

Fig. 4.1. Glass formation region in the system $PbO-TiO_2-(SiO_2+Al_2O_3)$

1.2. Crystallization Process of Glasses

The glasses were subjected to differential thermal analysis in order to determine their exothermal peak temperatures on heating. A piece of glass cut from the glass plates was put in a cylindrical hole (6mm in diameter and 14mm in height) of the DTA sample holder. The heating rate was 10°C/min. The α-Al_2O_3 was used as a reference material. Also the powder X-ray analysis was made of the glasses heated up to various temperatures. Some of the glasses exhibited opaque appearance as a result of heating up to just above the first exothermal peak. No crystalline diffraction line was detected, however, in their X-ray patterns, and the

opaqueness was attributed to occurrence of glassy two-phase separation. Such glasses were heated up to higher temperatures until the second exothermal peak was observed on the DTA curves and examined by X-ray diffraction.

The results of the DTA and X-ray analyses are summarized graphically in Fig. 4.2. The numbers in the figure refer to those of the glass compositions as designated in Table 4.1. The sign "S" in Fig. 4.2 refers to the exothermal peak temperature at which the glassy two-phase separation would have occurred. The sign "A" refers to the exothermal peak temperature at which the metastable lead titanate crystal of pyrochlore-type precipitated. This type of lead titanate was recently discovered by Martin[5] in the crystallized glasses of the system PbO-TiO_2-SiO_2-B_2O_3(or Na_2O). It was reported that this crystal dissolves a small amount of SiO_2 in it, although its exact chemical formula is not known. The sign "P" refers to the exothermal peak temperature at which the perovskite-type lead titanate crystal ($PbTiO_3$), a well known ferroelectric material, precipitated.

It can be seen from Fig. 4.2 that in general the crystallization starts at the temperatures ranging from 620° to 740°C, and the crystal precipitated first is either the lead titanate of the perovskite or pyrochlore type, or both.

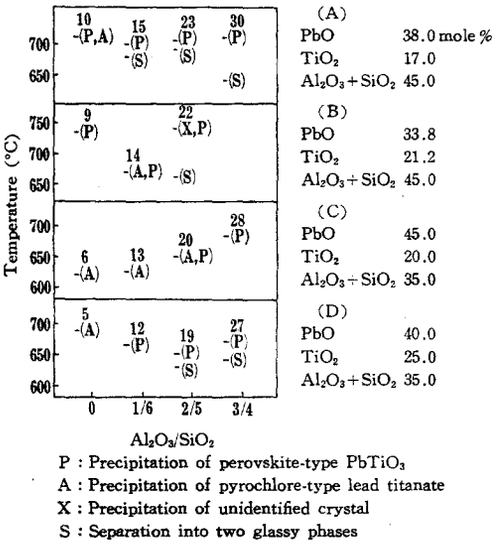

Fig. 4.2. Crystallization process of glasses.

1.3. Dielectric Properties of the Crystallized Glasses

The glass plates were cut into the form of slab, 2 by 10 by 10mm, placed on a platinum sheet and heat-treated in a SiC furnace on a schedule consisting of heating at a rate of 5°C/min from room temperature to the crystallization temperature and holding there for 1 hour, followed by cooling in the furnace. The first or second peak temperature on the DTA curves was taken as the crystallization temperature, according as crystallization of a glass took place at the first or second peak temperature.

Dielectric properties measured at room temperature and 1 Mc/s of the samples before and after the heat treatment are given in Table 4.2 together with the crystal phases identified by X-ray diffraction analysis in the heat-treated samples. For the measurement, a Q-Meter (Type GM-102, Yokogawa Electric Works, Ltd.) was used. The silver paste was applied on both faces of the samples as electrodes.

Table 4.2. Dielectric properties and crystal phases

Sample No.	Heat-treatment temperature (°C)	Dielectric properties				Crystal phases*
		Parent glass		Crystallized glass		
		ε	$\tan\delta \times 10^4$	ε	$\tan\delta \times 10^4$	
5	690	33	24	48	70	A,P
6	620	33	20	50	172	A
9	734	27	16	57	118	P
10	710	30	15	54	98	P,A
12	665	32	21	43	58	P
13	630	35	34	40	105	A
14	670	32	23	35	51	A,P
15	700	28	16	45	56	P
19	650	32	17	70	60	P
20	650	29	28	48	81	A,P
22	740	23	28	63	41	P,X
23	707	24	37	58	81	P
27	670	36	33	46	156	P
28	685	26	16	59	60	P
30	710	34	23	63	57	P

* A ; Pyrochlore-type lead titanate

P ; Perovskite-type $PbTiO_3$

X ; Unidentified crystal

It can be seen from Table 4.2 that for the present system, in general, both the dielectric constant and tanδ increase as a result of crystallization: The dielectric constant and tanδ of the samples before crystallization are in the range 23 to 36 and 0.0015 to 0.0037, respectively, whereas those after crystallization are in the range 35 to 70 and 0.0041 to 0.0172, respectively. Among the samples investigated, the composition No. 19 started to crystallize at a fairly low temperature, i.e. 650°C, giving a high dielectric constant of 70.

1.4. Dielectric Properties of the Crystallized Glass No. 19

In the following experiments, more precise examinations were made on the dielectric properties for the composition No. 19. The glass of the composition No. 19 was melted at 1250°C for 30min, poured on a steel plate, crushed to -100 mesh, and remelted at 1250°C for 30min to ensure thorough homogenization of the glass.

1.4.1. Effects of Heat Treatment

The glass was heated from room temperature to 650°C at a rate of 5°C/min, held at 650°C for various periods from 10 minutes to 9 hours, and then taken out of the furnace. Dielectric properties of the heat-treated glass samples measured at room temperature and 1 Mc/s are shown in Fig. 4.3. As can be seen from the figure, the dielectric constant reaches a definite value by the heat treatment within about three hours.

The effect of temperature of heat treatment on dielectric properties are shown in Fig. 4.4. The heat treatment consisted of heating from room temperature to 650°, 700°,

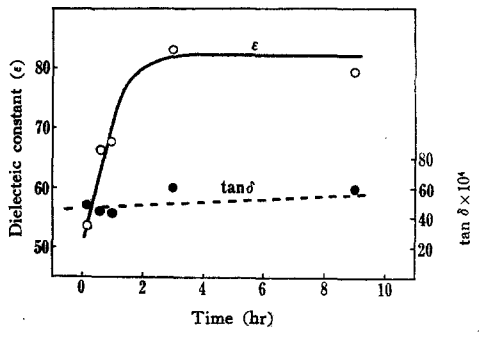

Fig. 4.3. Dependence of dielectric properties of the glass No. 19 upon heat-treatment period at 650°C.

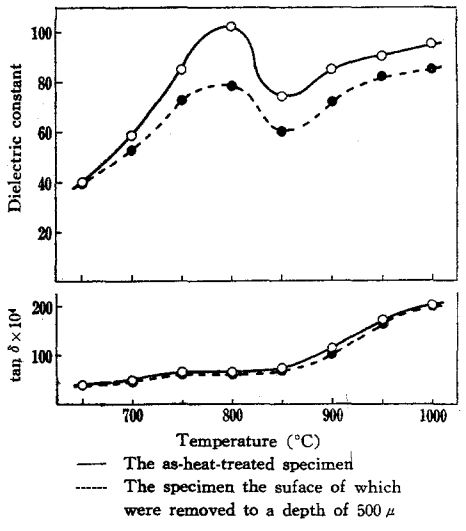

Fig. 4.4. Dependence of dielectric properties of the glass No. 19 upon heat-treatment temperature.

750°, 800°, 850°, 900°, 950° and 1000°C respectively at a rate of 5°C/min and taking out immediately from the furnace after the glass samples reached one of these temperatures. Solid lines refer to the results for the as-heat-treated samples whereas dotted lines refer to the results for those, both faces of which were removed to a depth of 500μ by grinding

with aluminum oxide powders after the heat treatment. It can be seen from the figure that the dielectric constant increases with increasing temperature of heat treatment in the range from 650° to 800°C, goes through a maximum at 800°C and then increases again above 850°C. The tanδ increases gradually in the range from 650° to 850°C and then more markedly up to 1000°C.

1.4.2. Dependence of Dielectric Properties on Temperature and Frequency of Measurement

A glass in the form of disk 40mm in diameter and 2mm thick was crystallized by heating from room temperature to 650°C at a rate of 5°C/min, holding at 650°C for 1hour and cooling in the furnace. Dielectric properties of the crystallized glass were measured, at 1 kc/s by using a transformers bridge (Type TRS-B, Ando Electric Co., Ltd.), during heating from room temperature to 180°C at a rate of 1°C/min. The result is shown in Fig. 4.5. The frequency dependence was measured at room temperature for another glass sample crystallized by the same heat treatment as described above. The result is shown in Fig. 4.6.

1.4.3. Effects of Sample Thickness

The dielectric properties described above are all for the samples approximately 2mm thick. It has been reported in Chapter 2 that some of ferroelectric glass-ceramics show lower values of dielectric constant when formed in a thinner sheet. In order to examine such dependence of dielectric properties on the sample thickness for the crystallized glass of the present system, the glass No. 19 was formed into a sheet 0.1mm thick and subjected to the same heat treatment

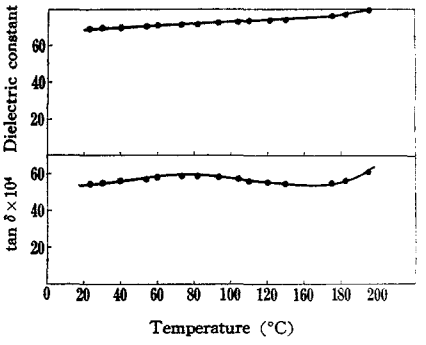

Fig. 4.5. Dependence of dielectric properties at 1 kc/s of the crystallized glass No. 19 upon temperature of measurement.

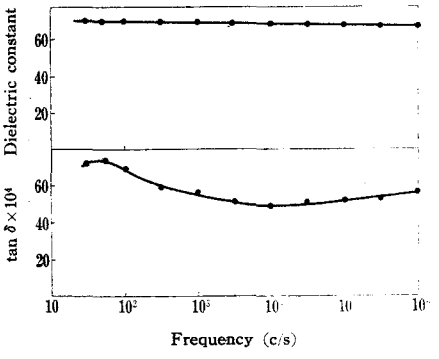

Fig. 4.6. Dependence of dielectric properties of the crystallized glass No. 19 upon frequency. The measurements were made at room temperature.

as described in paragraph 1.4.2. The method of forming the sheet was same as reported in Chapter 2. The dielectric constant and tanδ of the thin crystallized sheet measured at room temperature and 1 Mc/s were approximately 65 and 0.0070, resepectively, which were almost the same as obtained for the plate sample 2mm thick. That is, no appreciable effect of the sample thickness was found for the present crystallized glass.

1.5. Microstructure of the Crystallized Glass No. 19

1.5.1. Effects of Time of Heat Treatment

The crystal phase identified in the glasses heat-treated at 650°C for various periods (1.4.1.) was the perovskite-type $PbTiO_3$ crystal. Its amount was determined by X-ray analysis on the internal standard method: As the standard sample, a series of powder mixtures consisting of synthetic $PbTiO_3$ crystal and the glass of the composition No. 19 in various ratio and, in addition, fluorite, CaF_2, in a constant ratio to the total amount of the former two was prepared. From the X-ray patterns of these mixtures the ratios of the peak intensity for the (111) reflection of the sysnthetic $PbTiO_3$ crystals to that for the (111) reflection of the fluorite were determined, and from a relation between the peak intensity ratio and the synthetic $PbTiO_3$ crystal content a calibration curve for determination of the amount of the $PbTiO_3$ crystals in the crystallized glasses was prepared.

As is described later the $PbTiO_3$ crystals precipitated in the glass samples heat-treated at 650°C are cubic whereas the synthetic $PbTiO_3$ crystals obtained by sintering the mixtures of the Pb_3O_4 and TiO_2 crystal powders are tetragonal.

Therefore, as to the use of the synthetic $PbTiO_3$ crystal as a component of the standard samples, some discussions would be necessary on its appropriateness. The structure factor and multiplicity factor which affect the X-ray reflection intensity of crystal are the same for the (111) reflections of both of the crystals. Furthermore, the author has confirmed experimentally that the volume of their unit cells is almost the same. From these the author considered that reflections would be equal and consequently the use of the synthetic tetragonal $PbTiO_3$ crystals as a component of the standard materials would be justified.

The axial ratio (c/a) of the perovskite-type $PbTiO_3$ crystals was also determined from the position of the X-ray diffraction peaks for their (112) and (211) planes.

The results are given in Table 4.3, which indicates that the amount of the perovskite-type $PbTiO_3$ crystals increases with increasing time of heat treatment whereas their axial ratio (c/a) remains constant at one, irrespective of the time of heat treatment.

1.5.2. Effects of Temperature of Heat Treatment

The glasses crystallized by heating up to various temperatures ranging from 630° to 1000°C were subjected to the following examinations. The way of heating to each temperature and cooling was described in paragraph 1.4.1.

a) Observation by Metallurgical Microscope

The cross-sections of the heat-treated samples were observed by a metallurgical microscope. For each of the samples heat-treated below 750°C, no difference in texture was observed between its surface and interior, whereas for

Table 4.3. Crystal phase and its content in the glasses No. 19 heat-treated at 650°C for various periods

Time of heat treatment (hr)	Crystal phase	Axial ratio of $PbTiO_3$	Content of $PbTiO_3$ (wt %)
1/6	perovskite-type $PbTiO_3$	1.00	16
1/2	"	1.00	20
1	"	1.00	22
3	"	1.00	28
9	"	1.00	34

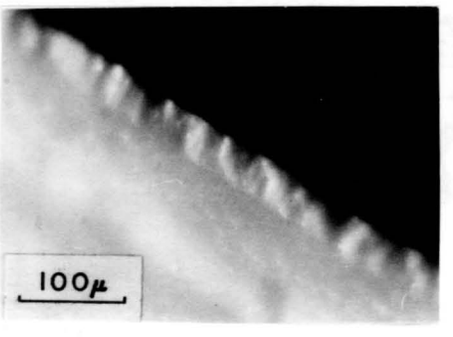

Fig. 4.7. Cross-section of the crystallized glass No. 19 heated up to 900°C.

those heat-treated above 800°C, needle-like crystals were observed in the vicinity of their surface. Fig. 4.7 is a micrograph of the cross-section of the sample heated up to 900°C. The thickness of the surface layer consisting of the needle-like crystals increases with increasing the heating temperature, reaching about 100μ at 1000°C.

b) Electron Microscopic Observation

The surface of the heat-treated glasses were ground to

a depth of 500μ and etched with 10 % HCl in various periods of 30 sec. to 5 min. at room temperature. Some of the electron micrographs of their chromium preshadowed carbon replicas are shown in Fig. 4.8.

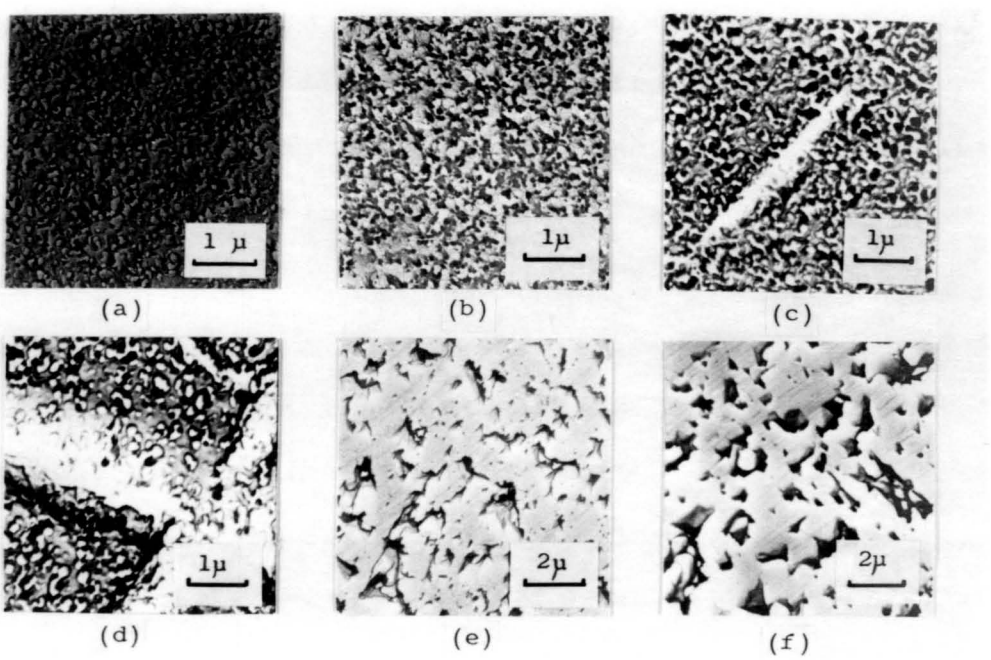

Fig. 4.8. Electron micrographs of the glass No. 19 heated up to 630°C (a), 800°C (b), 850°C (c), 900°C (d) 950°C (e) and 1000°C (f).

c) X-ray diffraction Analysis

The original surfaces of the samples and the surfaces ground to a depth of 500μ were X-rayed. The crystals identified were the perovskite-type $PbTiO_3$ crystal and the lead aluminum silicate crystal showing the same X-ray diffraction pattern as that already reported by Geller et al.[7] The former was found on both of the original and ground (interior) surfaces of the samples heat-treated above 650°C, whereas the latter only on the original surfaces of the

samples heat-treated above 800°C. The X-ray reflection intensities at d=2.30Å for the $PbTiO_3$ crystal and that at d=6.60Å for the lead aluminum silicate crystal, which are both indicative of the amount of the respective crystal, are plotted against the heating temperature of the samples in Fig. 4.9(a). The solid lines refer to the results for the original surfaces of the samples and the dotted lines refer to those 500μ beneath the original surfaces. Some new weak diffraction peaks, observed for the original surfaces of the samples heated above 950°C, were not shown in the figure.

In Fig. 4.9(b) are plotted the axial ratio (c/a) of the $PbTiO_3$ crystal against the heating temperature of the samples. The figure indicates that the perovskite-type $PbTiO_3$ crystal changes from cubic to tetragonal with increasing the heating temperature. This change occurs in the same way for both the original surface and the interior of the samples.

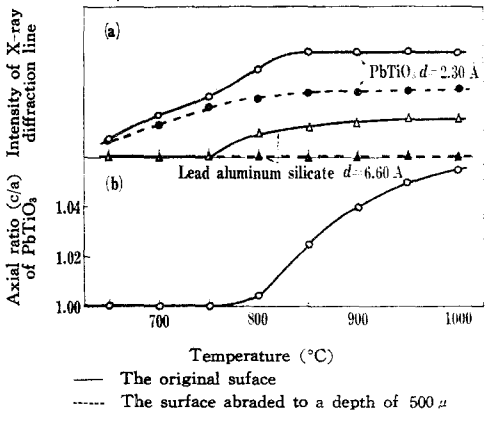

Fig. 4.9. Dependence of crystal content and axial ratio of $PbTiO_3$ in the glass No. 19 upon temperature of heat treatment.

2. Discussion

2.1. Glass Formation Region

It was shown in Chapter 1 that the glass formation region of the system BaO-TiO_2-SiO_2 broadened toward the higher concentration of the BaO and TiO_2 components when the SiO_2 was replaced with the Al_2O_3. In the present system PbO-TiO_2-SiO_2, however, the glass formation region was little affected by the replacement of the SiO_2 with the Al_2O_3. This may be attributed to the difference in charactor between the Ba^{2+} and Pb^{2+} ions: In BaO-TiO_2-SiO_2 glasses the Ba^{2+} ions behave as modifier ions, breaking the network of the glasses and so increase their tendency to devitrify. When the Al_2O_3 is added to the glasses in replacement of the SiO_2 new linkages are formed between the Al^{3+} ions and the singly-bonded oxygens formerly associated with the Ba^{2+} ions[8], and this improvement in the continuity of the network would lead to the broadening of the glass formation region. The Pb^{2+} ions in the glasses, however, behave in pairs as network-former ions[9], and the glass network in the system PbO-TiO_2-SiO_2 is considered to be so continuous already that there would be a almost no break in the network that needs the addition of the Al_2O_3 for its repair.

2.2. Crystallization Process of Glasses

2.2.1. Effects of Replacement of the SiO_2 with the Al_2O_3

It is seen from Fig. 4.2 that with the replacement of the SiO_2 with the Al_2O_3 the perovskite-type $PbTiO_3$ crystals tend to precipitate in place of the pyrochlore-type lead titanate. The precipitation of the pyrochlore-type lead

titanate crystals in PbO-TiO_2-SiO_2 glasses is reasonably expected because this type of lead titanate can contain the SiO_2 as a solid solution, becoming analogous in composition to their parent glass. It is likely that such crystals precipitate preferentially since the minimum atomic rearrangement and the minimum interface energy are involved in the transformation from glass to crystal.

On the other hand, if the glassy two-phase separation precedes the crystallization in the glasses to which Al_2O_3 was added and one of the separated phases is rich in PbO and TiO_2 components and poor in SiO_2 component, it would possible that the perovskite-type $PbTiO_3$ crsytals are formed instead of pyrochlore-type crystals. Russell et al.[2)3)] found a phase separation in a glass of the composition, PbO 34.7, TiO_2 17.3, Al_2O_3 10.9, SiO_2 37.1 by mole %, and, from the electron microscopic observation, reached the conclusion that the lead concentration in the dispersed droplets is much higher than that in their matrix and that the perovskite-type $PbTiO_3$ crystals precipitate within the dispersed droplets phase. Then it can be said tentatively that the addition of Al_2O_3 causes the two-phase separation leading to the preferential formation of the perovskite-type $PbTiO_3$ crystals.

2.2.2. Crystallization Process of the Glass No. 19

The crystallization of the glass No. 19 is considered to proceed as follows: The glass separates into two glassy phases (Fig. 4.2, No. 19) in the initial stage of heating; the dispersed droplets would be rich in PbO and TiO_2 and the matrix rich in SiO_2 and Al_2O_3. The size of the droplets

reaches 0.1 to 0.2μ in diameter near 630°C (Fig. 4.8(a)). At approximately 650°C the perovskite-type $PbTiO_3$ crystals start to form (Fig. 4.9) probably within the dispersed droplets and their formation continues up to approximately 850°C (Fig. 4.9). At approximately 800°C the lead aluminum silicate crystals start to precipitate probably in the glassy matrix rich in SiO_2 and Al_2O_3 (Fig. 4.9). They originate at the surface of the samples, growing inward (Fig. 4.7 and 4.9). At approximately 850°C the recrystallization of the $PbTiO_3$ crystals start to occur; aggregates of $PbTiO_3$ crystals in the form of convex lens as seen in the photographs of Fig. 4.8(c) and (d) are formed at the expense of the fine-grained $PbTiO_3$ crystals formerly precipitated in the dispersed glassy droplets. These aggregates grow and spread throughout the sample (Fig. 4.8(e) and (f)). The diameter of individual crystals composing the aggregate becomes finally 0.6 to 1.2μ. The crystallization process described above is represented schematically in Fig. 4.10.

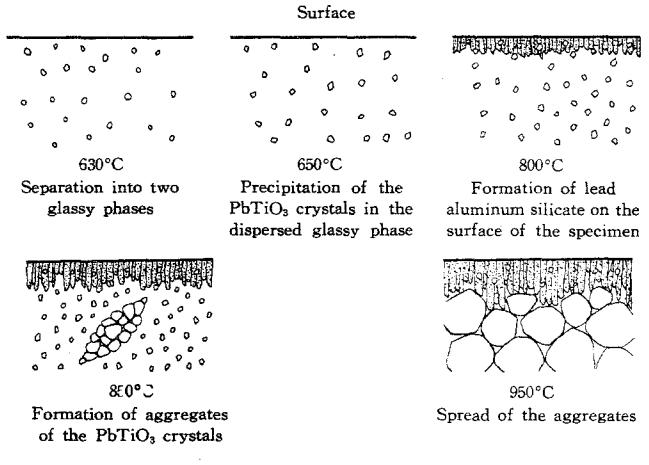

Fig. 4.10. Schematic representation of crystallization process of the glass No. 19.

2.3. Dielectric Properties of the Crystallized Glass No. 19 in Relation to Microstructute

As is shown in Fig. 4.3 the dielectric constant of the glass No. 19 heat-treated at 650°C increases with the time of heat treatment rapidly first and then reaches a constant value. In these glasses all crystals preciptated are of the perovskite-type with the axial ratio, c/a, equaling unity and therefore the change described above could be attributed only to the increase in amount of the $PbTiO_3$ crystals in the glasses. This can be confirmed if the dielectric constants of the glasses are plotted against the amount of the $PbTiO_3$ crystals by utilizing the data shown in Fig. 4.3 and Table 4.3. The relationship is almost linear as shown in Fig. 4. 11.

For those heat-treated up to various temperatures, however, the relationship between the dielectric constant and the amount of $PbTiO_3$ crystals precipitated is not simple,

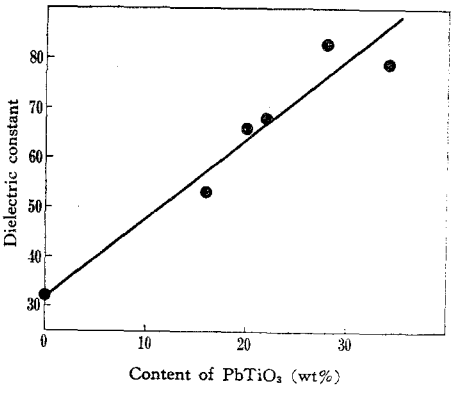

Fig. 4.11. Dielectric constant as a function of $PbTiO_3$ content.

because the size, distribution, structure etc. of the $PbTiO_3$ crystals which also affect the dielectric constant vary with the temperature of the heat treatment (Fig. 4.8 and 9). The following interpretation of the curves in Fig. 4.4 are based on the considerations of these factors.

The increase in dielectric constant with increasing the heating temperature from 650° to 750°C would simply be due to the increase in the amount of the $PbTiO_3$ crystals because in this temperature range no noticeable change in structure and size of the crystals was observed.

In the temperature range from 750° to 850°C the dielectric constant goes through a maximum and then decreases. As is seen in Fig. 4.9, lead aluminum silicate is formed on the surface of the sample above 800°C. Since the variation in dielectric constant above 750°C was also observed for the sample whose surface layer has been removed, some other causes of the variation in dielectric constant must be sought for. As seen from Fig. 4.8 and 9, the grain size of the $PbTiO_3$ crystals as well as the their axial ratio undergo great changes in this temperature range. It has been mentioned by Herczog[10] that the dielectric constant of the polycrystalline $BaTiO_3$ is largely affected by the size of their constituent crystal grains especially in the range from 0.1 to 10μ: At the grain size much larger than 1μ stresses are not produced in the crystal grains during their ferroelectric transition because it can be relaxed by domain wall motion in the grains. As the grain size becomes smaller and approaches 1μ, domain wall formation and motion become energetically unfavorable and the large stresses are induced

in the grains, resulting in the increase in dielectric constant of the material[11]. When the grain size becomes still smaller, the effect of a depolarized layer[12], which exists at surfaces of the particles and acts to lower the dielectric constant, becomes remarkable. Simultaneous presence of these two effects give rise to a maximum peak to appear at about 1μ of grain size in the curve illustrating the dielectric constant-grain size relationship. Although the reasoning mentioned above should be discussed further[13], the variation in dielectric constant with grain size itself has been experimentally confirmed for the polycrystalline $BaTiO_3$. For the polycrystalline $PbTiO_3$, such a relationship has not been established experimentally. Theoretically, however, it is highly probable that such a relation holds for the polycrystalline $PbTiO_3$ as well. If so, the peculliar change in dielectric constant in the temperature range from 750° to 850°C as observed in Fig. 4.4 could be understood: The increase in dielectric constant from 750° to 800°C would be due to the continued increase in the amount of the $PbTiO_3$ crystals as well as the decrease in the effect of the depolarized surface layer of their crystal grains. The decrease in dielectric constant above 800°C would be due to the predominance of the effect of the relaxation of the stresses in the grains resulted from grain growth. The change in the axial ratio of the $PbTiO_3$ beginning at 800°C (Fig. 4.9) is also attributed to the relaxation of the stresses in the grains.

The causes of the increase in dielectric constant over 850°C are not yet clear at present, but the two causes are

conceivable. The one is the connection of the fine grained $PbTiO_3$ crystals leading to the formation of the large crystal aggregates: The dielectric constant of the mixture consisting of the crystals with high dielectric constant and the glass matrix with low dielectric constant is low when the crystals are isolated by the glass matrix, but it increases when the crystals connect each other from one face to another face of the sample[14]. Another cause is the reduction of the Ti^{4+} ions to the Ti^{3+} ions in the sample, which seems to be indicated by the increase in the value of tanδ (Fig. 4.4). Which cause is predominant is the problem to be solved by further investigations.

3. Summary

1. The glass formation region was investigated of the system $PbO-TiO_2-Al_2O_3-SiO_2$ and the structural interpretaion was given.

2. The glasses prepared from this system began to crystallize at the temperatures 620° to 740°C and the crystals precipitated first were either the lead titanates of the perovskite or pyrochlore type, or both. The Al_2O_3 component in this system was found to promote the precipitation of the perovskite-type $PbTiO_3$ via the glassy two-phase separation.

3. The dielectric constant of the glass-ceramics prepared from the glasses of this system by the heat treatment at the temperatures from 620° to 740°C was in the range 30 to 70 at 10^6 c/s.

4. Detailed investigations on the dielectric properties were made for the glass-ceramics obtained by heating the glass

of the composition, PbO 40, TiO_2 25, Al_2O_3 10, SiO_2 25 by mole %, to various temperatures. The values of dielectric constant were correlated with their microstructures, especially, the amount of the $PbTiO_3$ crystals, axial ratio, grain size, continuity of the grains etc. The dielectric properties were not influenced by the sample thickness.

References

1) S.D. Stookey, U.S. Pat., 2,290,971, Jan. (1960).

2) C.K. Russell and C.G. Bergeron, J. Am. Ceram. Soc., 48 162 (1965).

3) C.K. Russell and C.G. Bergeron, J. Am. Ceram. Soc., 48 268 (1965).

4) C.G. Bergeron and C.K. Russell, J. Am. Ceram. Soc., 48 115 (1965).

5) F.W. Martin, Phys. Chem. Glasses, 6 143 (1965).

6) D.G. Grossman and J.O. Isard, J. Am. Ceram. Soc., 52 230 (1969).

7) R.F. Geller and E.N. Bunting, J. Res. Nat. Bur. Std., 31 266 (1943).

8) W.A. Weyl and E.C. Marboe, The Constitution of Glasses, Vol. II, Part 1, p. 508, Interscience Publishers, New York (1964).

9) M. Imaoka, J. Ceram. Assoc. Japan, 67 364 (1959).

10) A. Herczog, J. Am. Ceram. Soc., 47 107 (1964).

11) W. R. Buessem, L.E. Cross and A.K. Goswami, J. Am. Ceram. Soc., 49 33 (1966).

12) A. Anliker, H.R. Bruegger and W. Kaenzig, Helv. Phys. Acta, 27 99 (1954).

13) F.N. Bradley, J. Am. Ceram. Soc., 51 293 (1968).

14) W.D. Kingery, Introduction to Ceramics, p. 719, John Wiley & Sons, inc., New York (1960).

Chapter 5. Preparation and Properties of the Thick-Film Glass-Ceramics

One of the potential practical applications of high dielectric constant glass-ceramics is the use as capacitor component for print circuits. For such an application, glasses should be applied on substrates and crystallized in situ, instead of being applied in the form of finished glass-ceramic plates or sheets. In other words, the technique of "thick-film", where fine-grained glass powder is printed on the substrate and then fired, would be most appropriate. In this chapter, a detailed description is presented on the thick-film capacitors made from the glasses in the systems $PbO-TiO_2-SiO_2$ and $PbO-TiO_2-Al_2O_3-SiO_2$ with or without small amounts of other components. Powders of the glasses, if applied on substrate and fired, are expected to soften at fairly low temperatures and simultaneously crystallize into high dielectric constant films. The variation of the dielectric properties is discussed in terms of microstructure of the capacitors.

Asher et al.[1] reported briefly the properties of thick-film capacitor based on glass-ceramics. Any details on the chemical composition and the effect of microstructure on the dielectric properties, however, were not given, and the basic problems in application of glass-ceramics to thick-film capacitor is left to be studied.

1. Experimental

1.1. Fabrication of Thick-Film Capacitors

1.1.1. Preparation of Glass Powders to be Used as Capacitor Dielectrics

Glasses in the system PbO-TiO_2-SiO_2 and PbO-TiO_2-Al_2O_3-SiO_2 with or without some small amounts of other components were melted for use as the capacitor dielectrics. The compositions of the glasses are shown in Table 5.1. All the batch materials used were reagent grade chemicals.

Table 5.1. Glass compositions

Sample No.	Composition (mole %)					
	PbO	TiO_2	SiO_2	Al_2O_3	B_2O_3	Other component
1	33.8	21.2	45.0			
2	38.0	17.0	45.0			
3	40.0	25.0	35.0			
4	45.0	20.0	35.0			
5	33.8	21.2	32.1	12.9		
6	38.0	17.0	32.1	12.9		
7	40.0	25.0	25.0	10.0		
8	45.0	20.0	25.0	10.0		
9	45.0	25.0	15.0	10.0	5.0	
10	45.0	25.0	12.0	10.0	8.0	
11	42.0	25.0	15.0	10.0	5.0	PbF_2 2, ZnO 1
12	42.0	25.0	15.0	10.0	5.0	PbF_2 1, ZnO 1, K_2O 1

About 50g of the mixed batch materials were put in a platinum-10% rhodium crucible of 50cc in capacity, covered with a lid, and melted at 1250°C for 45 minutes. The melts were poured on a stainless steel plate and pressed with another piece of steel plate. The glasses thus obtained were crushed and powdered to -325 mesh.

1.1.2. Application of Glass Powders and their Firing

Thick-film capacitors were fabricated by the process shown in Fig. 5.1. Plates of 92 % sintered alumina, about 0.6mm in thickness, were used as substrates. Palladium paste, which consisted of 96 weight % palladium powder, 4 weight % lead-borosilicate glass powder and alkyd varnish (0.3cc per 1g of the two powders), was used to form the bottom conductor. The paste was apllied by brushing on the substrate in the form of a disc about 10mm in diameter and 4μ thick, and after drying, fired with the following heating schedule; 5°C/min to 850°C, 10 minutes' holding and cooling in the furnace.

Glass powder paste for capacitor dielectrics was prepared by mixing 1g of the glass powder and 0.3cc of alkyd varnish. The paste was applied by brushing over the bottom conductor in the form of a disc about 12mm in diameter and 100μ thick. After drying of the paste, the wafer was heated, at a rate of 5°C/min, to a temperature between the lowest exothermal temperature of the glass used and the highest temperature at which a unifom dielectric film could be obtained. Immediately after the given temperature was reached, the wafer was taken out of the furnace. The lowest exothermal temperatures of the glasses had been determined by

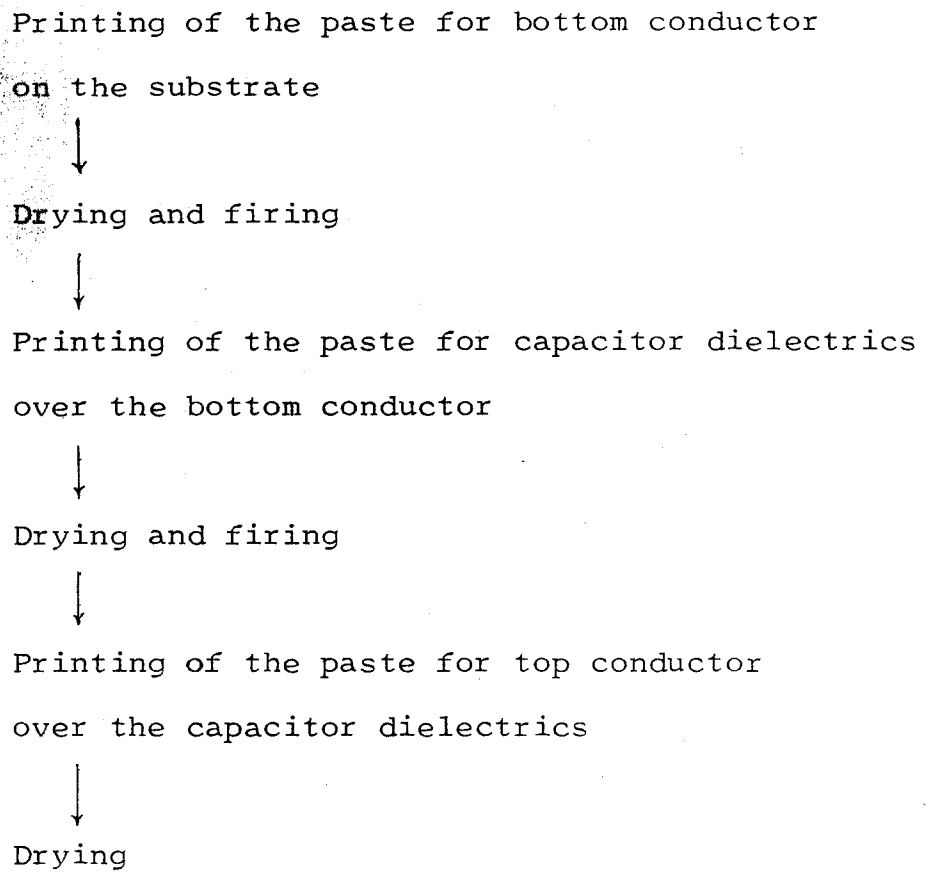

Fig. 5.1. Fabrication process of thick-film capacitor.

the differential thermal analysis. The exotherms observed for the present systems are attributed to the glassy two-phase separation or precipitation of lead titanates of the perovskite or pyrochlore type, as already reported in Chapter 4. When the substrate with the glass powder paste applied was heated over the highest temperature mentioned above, formation of many bubbles in the dielectric film or penetration of the fluid glass into the alumina substrate was observed. The heating at a rate higher than 5°C/min often caused pin holes or fissures in the dielectric film. Rate of cooling after firing did not give any appreciable effect on the properties of dielectrics.

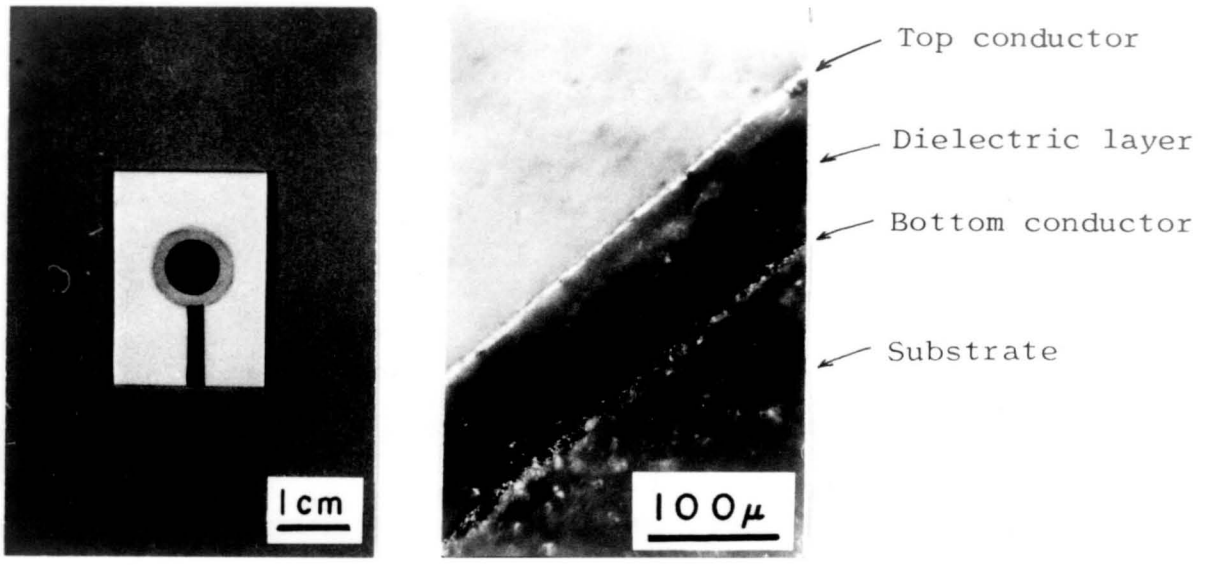

Fig. 5.2. Appearance of the thick-film capacitor.

As a top conductor, silver paste was applied over the dielectric film and dried by heating at about 200°C. The overall appearance and cross-section of the thick-film capacitor thus obtained are shown in Fig. 5.2.

1.2. Dielectric Properties of Thick-Film Capacitors

Dielectric constant and tanδ, both measured at a frequency of 1 Mc/s, of the thick-film capacitors are shown in Fig. 5.3, 4 and 5 as functions of firing temperatures. The measurements were made at room temperature by a Q-meter (Type GM-102, Yokogawa Electric Works, Ltd.). The numbers in the figures refer to those of the glass compositions as designated in Table 5.1.

These figures show that dielectric constant and tanδ of the thick-film capacitors range from 12 to 94, and from 0.0034 to 0.00280, respectively. It is also seen that high

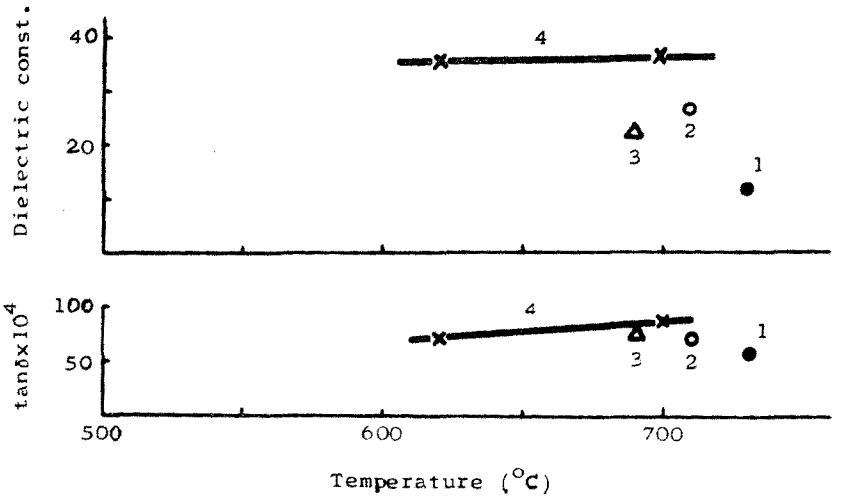

Fig. 5.3. Dielectric properties of thick-film capacitors as functions of firing temperature.

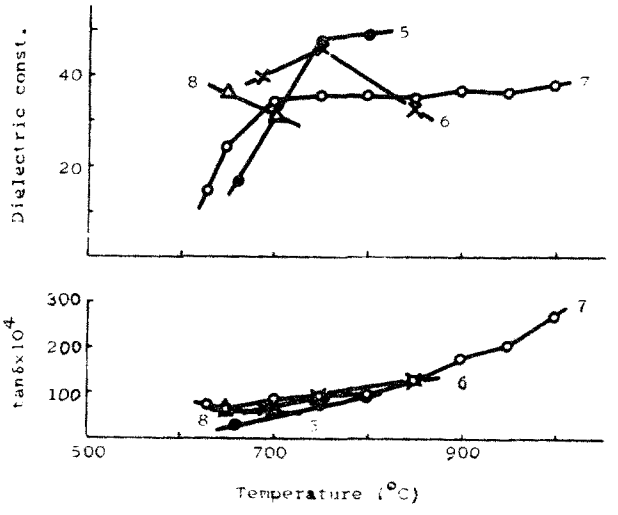

Fig. 5.4. Dielectric properties of thick-film capacitors as functions of firing temperature.

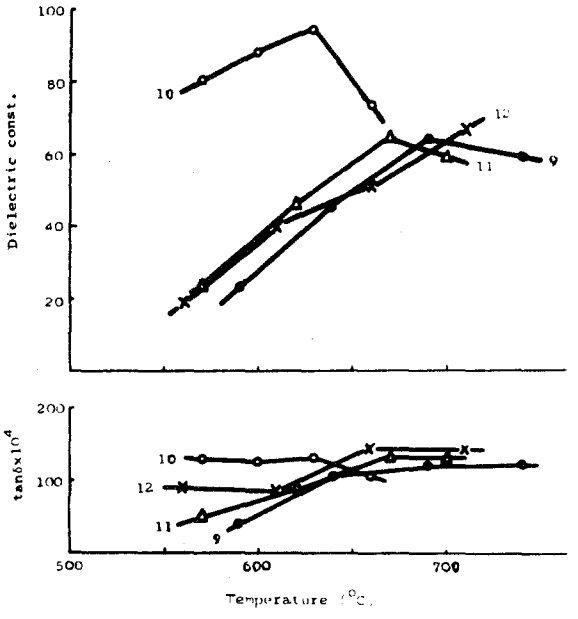

Fig. 5.5. Dielectric properties of thick-film capacitors as functions of firing temperature.

dielectric constant capacitors can be obtained with glasses containing B_2O_3 (No. 9 to 12).

The temperature dependence of the dielectric properties of the thick-film capacitor No. 10 are shown in Fig. 5.6.

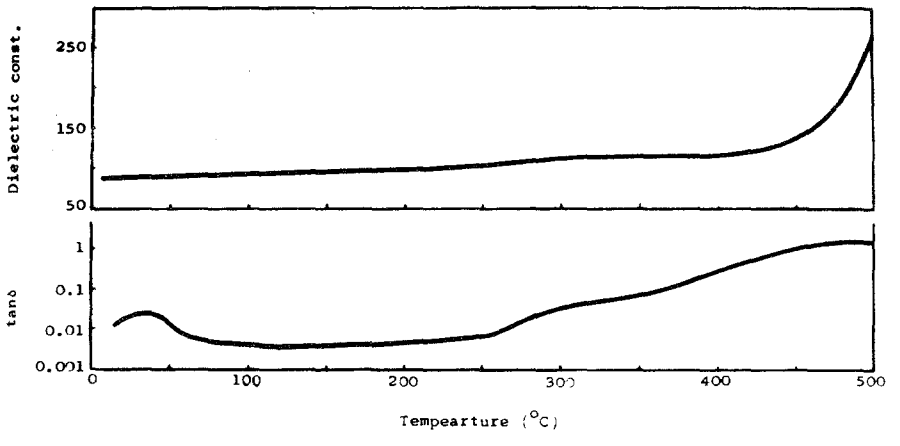

Fig. 5.6. Dependence of dielectric properties, at 1 kc/s, of the thick-film capacitor No. 10 upon temperature of measurement.

The capacitor was obtained by firing to 630°C. The measurements were conducted at 1 kc/s by a transformers bridge (Type TRS-B, Ando Electric Co., Ltd.). The figure shows that the dielectric constant changes linearly with temperature from room temperature to 270°C with a temperature coefficient of 0.00083/degree.

1.3. Comparison of Dielectric Properties of Thick-Film Dielectrics with Those of Bulk Glass-Ceramics

The dielectric properties at 1 Mc/s (measured at room temperature) of the thick-film dielectrics applied on the alumina substrates and fired to various temperatures were compared with those of the bulk glass-ceramics of the compositions No. 7 and 10. The dielectric properties of the bulk glass-ceramics were measured with the plate samples about 2mm thick. Silver paste applied on both surfaces of the glass-ceramics were used as the electrodes. In Fig. 5.7 the results are shown as functions of the temperature of heat treatment.

It is seen from the figure that for the composition No. 7 the dielectric constants of the thick-film dielectrics are much lower than those of the bulk glass-ceramics irrespective of their heat-treatment temperatures, whereas the difference in dielectric constant is not so large for the composition No. 10.

1.4. Microstructure and Dielectric Properties

To find the reason for the difference in dielectric constant between the thick-film dielectrics and bulk glass-ceramics, a number of experiments were made with the compositions No. 7 and 10. The dielectric properties and micro-

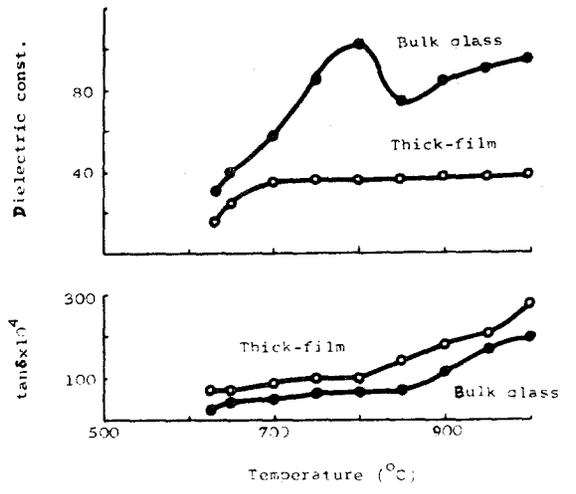

(a) Composition No. 7

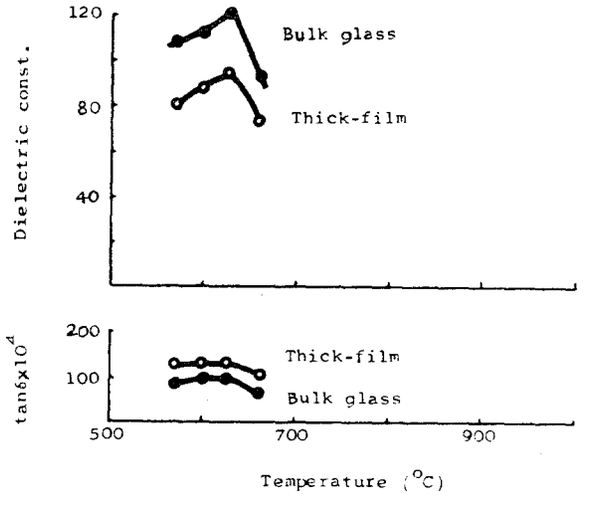

(b) Composition No. 10

Fig. 5.7. Dielectric properties of thick-film dielectrics and glass-ceramic plate as functions of temperature of heat treatment.

structure of the bulk glass-ceramics of the composition No. 7 have been given in Chapter 4.

1.4.1. X-Ray Diffraction Analysis

The virgin surfaces of the thick-film dielectrics of the composition No. 7 and 10 formed on the alumina substrates by firing at 750° and 630°C, respectively, were examined by X-ray diffraction method. For comparison, X-ray analysis was also made on 2mm thick plates of glasses which were crystallized by the same heat treatment. The results are shown in Table 5.2. The crystal identified, its axial ratio (c/a) and orientation of the crystallites are the same for both the thick-film dielectrics and bulk glass-ceramics. Also the amount of crystals precipitated are almost the same for each composition. It should be noted that the same value of the axial ratio means the same size of the crystal grains. It was shown in Chapter 4 that the former varies with the latter.

It was also confirmed by X-ray analysis of the thick-film dielectrics ground to varying depths that $PbTiO_3$ is the only crystalline speies at the interface between the glass layer and palladium layer as well as in the interior.

1.4.2. Observation by Metallurgical Microscope

The surface of the thick-film dielectrics of the compositions No. 7 and 10 formed on the alumina substrates by firing to 750° and 630°C, resepectively, were observed by a metallurgical microscope and compared with the surfaces of the 2mm thick crystallized glass plates. The microphotographs of the thick-film dielectrics are shown in Fig. 5.8. It is seen that the surface of the thick-film dielectrics

Table 5.2. Results of the X-ray diffraction analysis

Sample		Identified crystal	$PbTiO_3$ Axial ratio	$PbTiO_3$ Amount*	$PbTiO_3$ Preferred orientation
No. 7	Crystallized glass plate	Perovskite-type $PbTiO_3$	1	100	Not detected
	Thick-film dielectrics	〃		87	〃
No.10	Crystallized glass plate	〃		100	〃
	Thick-film dielectrics	〃		93	〃

* Amount of the $PbTiO_3$ crystal indicated by the relative intensity of a diffraction line for (111) plane. The intensity for each of the crystallized glass plates was taken as 100.

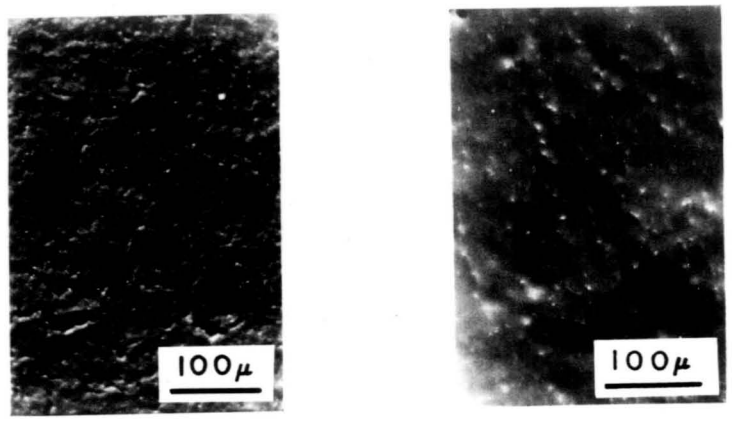

Composition No. 7 fired to 750°C

Composition No. 10 fired to 630°C

Fig. 5.8. The surfaces of the thick-film dielectrics.

No. 10 is fairly smooth whereas that of No. 7 has many small cracks. On the other hand, the crystallized glass plates of both the compositions had very smooth surfaces.

1.4.3.Texture of Thicker Dielectrics

Thicker dielectric films (about 0.6mm thick) of the composition No. 7 were prepared on the substrate by firing to 590°, 610°, 650° and 1000°C, respectively. Also those of No. 10 were prepared by firing to 510°, 530°, 570° and 630°C, respectively. Photographs of the resultant wafers are shown in Fig. 5.9. It is seen that large cracks are formed in the dielectric films No. 7 as a result of heating at relatively low temperatures and the width of cracks increases with increasing temperature. On the other hand, such large cracks are not seen in the dielectric film No. 10. In a separate observation, it was confirmed that in the film No. 7 cracks were formed in the firing process but not in the cooling process.

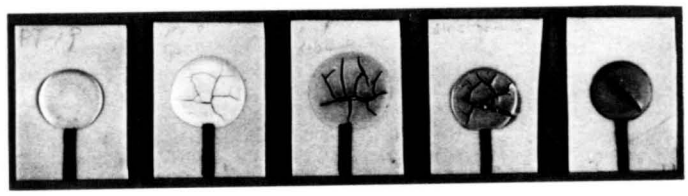

(a) Composition No. 7

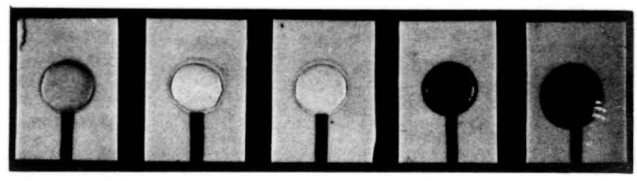

(b) Composition No. 10

Fig. 5.9. Appearances of the thicker dielectrics formed on the substrates.

1.4.4. Glass-Ceramics Prepared by Sintering Glass Powder without Use of Substrate

Glass powder pastes for the capacitor dielectrics of the compositions No. 7 and 10 were cast into a mold of filter-paper (0.5mm in depth and 20mm in diameter), and the resultant discs were fired at 750° and 630°C, respectively. Silver paste was applied on both surfaces of the fired samples as electrodes. The room temperature dielectric constant and tanδ measured at 1 Mc/s were 70 and 0.0138 for the composition No. 7, and 99 and 0.0092 for the composition No. 10, respectively. These values are nearly equal,

respectively, to those (Fig. 5.7) of the 2mm thick glass-ceramics of the same composition.

1.4.5. Crystallization of Thin Glass Sheet with Pd Paste

Thin glass sheets (0.1mm in thickness) of the composition No. 7 and 10 were crystallized by heating, respectively, at 850° and 630°C after palladium paste was applied to one surface of each sheet. The other surface was painted with silver paste after the crystallization. The dielectric constant and tanδ of the glass-ceramics thus obtained were, respectively, 71 and 0.0162 for the composition No. 7 and 100 and 0.0060 for No. 10. Comparison of these values with those in Fig. 5.7 for the 2mm thick glass-ceramics shows that the similar dielectric constants are obtained in both the cases, if composition of the glass and heating schedule are the same. As described in paragraph 1.3, palladium paste was not applied to the 2mm thick glass-ceramics.

2. Discussion

In the experimental part (1.3), it was found that the dielectric constant of the thick-film dielectrics formed on an alumina substrate is much lower than that of the bulk glass-ceramics, when the glass of the composition No. 7 is used. This can not be attributed to pores which might have been formed in the thick-film dielectrics in the course of sintering of glass powder, because the glass-ceramic produced by sintering glass powder exhibits the similar dielectric constant as the glass-ceramic produced from the bulk glass (1.4.4.). It is not likely that the kind, amount, size and orientation of the crystals precipitated in the film

are main factors which lower the dielectric constant of the thick-film dielectrics, since no appreciable difference in such characteristics was found between the thick-film dielectrics and the bulk glass-ceramics (Table 5.2). As to the reaction of the thick-film with palladium bottom conductor as a possible cause for lowering of the dielectric constant of the thick-film dielectrics, X-ray diffraction analysis did not reveal any evidence of the presence of reaction products (1.4.1). Actually, the thin glass-ceramics, to which palladium paste was applied before heat treatment, did not show any decrease in dielectric constant (1.4.5).

The most probable cause of the low dielectric constant of the thick-film dielectrics No. 7 would be the cracks. Presence of cracks in the thinner film of dielectrics was confirmed by microscopic examination (Fig. 5.8(a)). And severer cracks were found in the thicker film (Fig. 5.9(a)). Detailed inspection of Fig. 5.9(a) leads us to assume that some of the cracks make a laminar structure in the dielectrics. If so, the cracks will reduce the apparent dielectric constant of the thick-film dielectrics drastically[2)], because the film of dielectrics is divided into a number of sheets, between which there are thin voids. On the other hand, no decrease in dielectric constant was observed when the glass No. 10 was used for making the thick-film dielectrics. This corresponds to the fact that in this case no crack was detected both in the thinner film and thicker film.

As described previously (1.4.3), the cracks in the dielectric film (No. 7) were formed during the firing process, not during the cooling process. Therefore, it is supposed

that the formation of cracks is caused by the shrinkage of a layer of glass powder; the layer of glass powder shrinks on firing due to the tendency of the glass powder to adhere to each other. At the same time, the glass powder tends to adhere to the surface of the substrate which expands on firing. Thus crack formation is possible to occur at the weak sites in the layer of glass powder. The cracks once formed do not disappear on further firing to higher temperatures since the glass powder begins to crystallize, which prevents softening of the glass layer. This would be the case for the glass of the composition No. 7. In contrast to this glass, the glass No. 10 does not crystallize easily and, therefore, softens without forming cracks before crystallization. As a result, a uniform dielectric film is formed. Such glass powder should be suitable for making the capacitor dielectrics.

3. Summary

1. A thick-film cpacitor having a dielectric constant of 94 and tanδ of 0.0130 (at 10^6c/s) was obtained by firing powder of a $PbO-TiO_2-Al_2O_3-SiO_2-B_2O_3$ glass on a alumina substrate to approximately 600°C. The layer of glass powder was changed to a glass-ceramic film in this firing process. The temperature dependence of the dielectric constant of the capacitor was almost linear in the range from room temperature to 270°C with temperature coefficient of 0.00083/degree.

2. It was found that glass powders which soften before crystallization are suitable for preparing capacitors of high dielectric constant. Otherwise, many cracks were

formed in the thick-film dielectrics, which resulted in the lowering of its apparent dielectric constant.

Refernces

1) J.W. Asher and C.R. Pratt, Jr., Proc. Elec. Component Conf., 239 (1968).

2) W.D. Kingery, Introduction to Ceramics, p. 719, John Wiley & Sons. Inc., New York (1960).

H.H. Nester and T. Cocca, Ceramic Age, 84 (9) 38 (1968).

SUMMARY

For the purpose of finding the principles underlying the preparation of high dielectric constant ceramics via crystallization of glass, glass formation tendency, crystallization process of glass and the dielectric properties of the crystallized glass in relation to its microstructure were investigated for the bulk, thin sheet and thick-film samples in the system $BaO-TiO_2-Al_2O_3-SiO_2$ and $PbO-TiO_2-Al_2O_3-SiO_2$.

Part I (Chapter 1 to 3) was concerned with the $BaO-TiO_2-Al_2O_3-SiO_2$ glasses which precipitated barium titanate $BaTiO_3$, one of the most popular ferroelectric crystals.

In Chapter 1, general informations on the glass formation region, crystallization behavior of glasses and dielectric properties of crystallized glasses were presented, for the system $BaO \cdot TiO_2-Al_2O_3-SiO_2$, as summarized as follows:

1. Glasses richer in BaO and TiO_2 components can be prepared in the system $BaO \cdot TiO_2-Al_2O_3-SiO_2$ than in the $BaO \cdot TiO_2-SiO_2$.
2. Upon reheating of the glass, both $BaTiO_3$ ferroelectric crystals and non-ferroelectric crystals are precipitated. The amount of the $BaTiO_3$ crystal, however, increases as the temperature of heat treatment is raised. The amount of the $BaTiO_3$ crystal precipitated in the final products depends not only on the content of the BaO and TiO_2 components in the parent glass but also on the Al_2O_3/SiO_2

mole ratio. Crystallized products obtained from the glasses containing too much amount of $BaO \cdot TiO_2$ or Al_2O_3 show defects such as cracks and surface ripples.

3. As the glass is crystallized, the dielectric constant increases greatly. The dielectric constant of crystallized glass increases with increasing volume fraction of $BaTiO_3$ crystal in accordance with a Braggeman's mixture rule for porphyritic mixture.

In the practice, high dielectric constant ceramics are often used in the form of thin sheet, for example, as the capacitor. In Chapter 2, method for preparing thin sheet glass-ceramics in the system $BaO \cdot TiO_2$-Al_2O_3-SiO_2 and their dielectric properties were dealt with, and the following informations were obtained:

1. Thin sheet glass-ceramics 50-100μ thick can be prepared by a method which comprises squeezing the molten glass by the drams of solid cast iron and subjecting the produced glass sheets to heat treatments.
2. Glasses richer in BaO and TiO_2 components can be obtained as a result of rapid cooling when the above method is employed.
3. The thin sheet glass-ceramic shows a dielectric constant about a half of that of the bulk sample when its thickness is less than 200μ. It is attributed to a preferred orientation of hexacelsian ($BaAl_2Si_2O_8$) precipitated near the surface of the crystallized glass.

In Chapter 3, crystallization process of the $BaO \cdot TiO_2$-Al_2O_3-SiO_2 glass was dealt with in detail in order to find the cause of preferred orientation of the hexacelsian

crystals, and the following informations were obtained:

1. The crystallization process at the surface of the glass is different from that in the interior; near the surface of the glass, a metastable crystal is formed first and then it transforms progressively to the stable $BaTiO_3$ and hexacelsian, whereas in the interior the $BaTiO_3$ and hexacelsian are formed together originally.
2. Presence of the preferred orientation of hexacelsian in the crystallized products is attributed to the preferred orientation of the metastable crystal and the resemblance of the structure between the metastable crystal and hexacelsian.

Part II (Chapter 4 and 5) was concerned with the PbO-TiO_2-Al_2O_3-SiO_2 glasses which precipitated lead titanate $PbTiO_3$, a high Curie temperature ferroelectric crystal.

In Chapter 4, glass formation, crystallization behavior of glasses and the dielectric properties of crystallized glasses were presented for the system PbO-TiO_2-Al_2O_3-SiO_2, as summarized as follows:

1. The glass formation region in this system is little affected by the replacement of the SiO_2 with Al_2O_3.
2. The glasses of this system crystallize at the temperatures much lower than those of the system BaO-TiO_2-Al_2O_3-SiO_2.
3. Upon reheating of the glass, lead titanates of perovskite or pyrochlore type are precipitated. The Al_2O_3 component promotes the precipitation of the perovskite-type $PbTiO_3$ crystal via the glassy two-phase separation.

4. The amount of $PbTiO_3$ crystal precipitated increases as the temperature of heat treatment is raised. Various structural changes, such as precipitation of non-ferroelectric crystals, grain growth, change of the axial ratio and interconnection of the $PbTiO_3$ crystal, also occur as functions of the temperature of heating.
5. The dielectric constant of the crystallized glass is drastically influenced by the grain size and continuity of the $PbTiO_3$ crystals etc. as well as their content.
6. The dielectric constant of the crystallized glass of this system is not influenced by the sample thickness.

One of the potential practical applications of high dielectric constant glass-ceramics is the use as capacitor component for print circuits. In Chapter 5 the dielectric properties of the thick-film capacitors made from the glass-ceramics in the system $PbO-TiO_2-Al_2O_3-SiO_2$ were presented, as summarized as follows:

1. The $PbO-TiO_2-Al_2O_3-SiO_2-B_2O_3$ glass powder, if applied on substrate and fired, soften at fairly low temperature and simultaneously crystallize into high dielectric constant film. The temperature dependence of the dielectric constant of the film is small and linear up to fairly high temperature.
2. Glass powders which soften before crystallization are suitable for preparing thick-film capacitors of high dielectric constant. Otherwise, many cracks are formed in the thick-film dielectrics, which results in the lowering of its apparent dielectric constant.

ACKNOWLEDGEMENTS

The author wishes to acknowledge the guidance and encouragement of Professor M. Tashiro throughout this work. He is also very grateful to Professor S. Sakka for his helpful suggestions rendered during the course of the studies. Messrs. C. Kung and H. Nagao also contributed with many experimental works and useful discussions. The author would also like to express appreciation to Mr. Tamaki for his assistance in the experimental works. Appreciation is also extended to all the staff at the Laboratory of Ceramic Chemistry, Institute for Chemical Research, Kyoto University.